QUANTIFYING PRODUCED AND INJECTED WATER VOLUMES

IN SOUTHEASTERN SASKATCHEWAN

A Thesis Submitted to the
College of Graduate and Postdoctoral Studies
In Partial Fulfillment of the Requirements
For the Degree of Master of Science
In the Department of Civil, Geological, and Environmental Engineering
University of Saskatchewan
Saskatoon

By

Keegan Jellicoe

PERMISSION TO USE

In presenting this thesis/dissertation in partial fulfillment of the requirements for a Postgraduate degree from the University of Saskatchewan, I agree that the Libraries of this University may make it freely available for inspection. I further agree that permission for copying of this thesis/dissertation in any manner, in whole or in part, for scholarly purposes may be granted by the professor or professors who supervised my thesis/dissertation work or, in their absence, by the Head of the Department or the Dean of the College in which my thesis work was done. It is understood that any copying or publication or use of this thesis/dissertation or parts thereof for financial gain shall not be allowed without my written permission. It is also understood that due recognition shall be given to me and to the University of Saskatchewan in any scholarly use which may be made of any material in my thesis/dissertation.

Requests for permission to copy or to make other uses of materials in this thesis/dissertation in whole or part should be addressed to:

Head of the Department of Civil, Geological and Environmental Engineering

University of Saskatchewan

57 Campus Drive

Saskatoon, Saskatchewan, S7N 5A9, Canada

OR

Dean

College of Graduate and Postdoctoral Studies

University of Saskatchewan

116 Thorvaldson Building, 110 Science Place

Saskatoon, Saskatchewan, S7N 5C9 Canada

ABSTRACT

Large volumes of often saline formation water are both produced from and injected into sedimentary basins as a by-product of oil and gas production. Despite this, the distribution and interactions of water production and injection wells have not been studied in detail, and the effects of long-term water injection on reservoir pressures and groundwater quality remain uncertain. Even where injection and production volumes are equal at the basin scale, local changes in hydraulic head can occur due to the distribution of production and injection wells. These changes in hydraulic head are important in understanding induced seismicity and can potentially act as drivers of saline fluid flow, possibly leading to contamination of overlying potable groundwater resources where high permeability pathways are present. Across the Western Canada Sedimentary Basin (WCSB), approximately 29 km^3 of water has been co-produced with oil and gas, and 30 km^3 of water has been injected into the subsurface for saltwater disposal or enhanced oil recovery (EOR). This study evaluates the effects of production and injection wells on deep groundwater resources by examining wells within the southeastern WCSB. A comprehensive fluid budget was created for each formation, as well as maps of the spatial distribution of produced and injected water within each formation. By comparing spatial distributions and formation fluid budgets, it was possible to locate areas where high levels of injection pose the most substantial risk of contamination. In the Midale Member, areas with high injection volumes were found to be injecting at rates up to 6,000 times that of the estimated natural formational flow rate. Modelled pressures changes in the Midale Member were found to exceed >8 MPa at up to 250 m away from the injection well, and 2 MPa at up to 1.5 km away, which translates to hydraulic head values above the ground surface and may potentially lead to upward leakage of fluids in the presence of permeable pathways. Increased formation pressures due to injection are not unique to the southeastern WCSB and have been recorded in several other regions including Oklahoma, Texas, and Kansas, in some cases leading to induced seismicity. While many of these settings have small changes in the overall fluid budgets, the distribution of production and injection wells can cause substantial changes to fluid pressures locally.

ACKNOWLEDGEMENTS

I would like to thank my supervisors, Dr. Grant Ferguson and Dr. Jennifer McIntosh for their amazing support throughout my thesis. They provided me with invaluable guidance on the technical aspects of this project as well as continuous assistance with the editing of the thesis. I would also like to extend thanks to the rest of the Saskatoon-Tucson research group for all the great conversations whether it was in Phoenix or over Zoom.

TABLE OF CONTENTS

LIST OF TABLES

LIST OF FIGURES

1. Introduction

The continuing rise of oil and gas production has intensified water usage (Horner et al. 2016; Kondash et al. 2018), leading to an increase in discussion of related water management issues, including growing volumes of produced water (Scanlon et al. 2017; Tiedeman et al. 2016; Lutz et al. 2013), and groundwater contamination concerns due to hydraulic fracturing and saltwater disposal (Vengosh et al. 2014; Warner et al. 2013). Produced water represents the largest by-product of oil and gas production, and in 2017 the total volume of produced water in the US exceeded 3.8 billion m^3 (Veil 2020). These large volumes of produced water have prompted several studies over the last decade into water intensity (Scanlon et al. 2014, 2017; Ferguson 2015; McIntosh and Ferguson 2019). It is estimated that 91.5% of this produced water is managed by subsurface injection (Veil 2020) via saltwater disposal or for enhanced oil recovery (EOR). In addition, substantial volumes of surface water or shallow groundwater are reinjected into the subsurface leading to a surplus of water in several basins (Scanlon et al. 2017; Veil 2020; McIntosh and Ferguson 2019; Murray 2013). A surplus of water due to extensive injection can lead to increased reservoir pressures driving solute transport (McIntosh and Ferguson 2019) and, in some cases, induced seismicity (Keranen and Weingarten 2018).

Despite the shifting focus to produced water volumes within the oil and gas industry, there has been little discussion into the spatial distributions of fluids that are being produced and injected. Previous studies have found injected and produced volumes to be similar (Ferguson 2015; McIntosh and Ferguson 2019; Clark and Veil 2009), but injection and production locations have not been studied in detail. Even where injection and production volumes are equal at the basin scale, local changes in the hydraulic head will occur due to the distribution of production and injection wells. These changes are potentially important drivers of fluid flow and could lead to contamination of overlying freshwater resources where high permeability pathways are present (McIntosh and Ferguson 2019). The distribution of production and injection wells, associated changes in local fluid budget, and effect on porewater pressure are also important in understanding induced seismicity (National Research Council 2013; Rubinstein and Mahani 2015; Keranen and Weingarten 2018). Additionally, changes in subsurface pressures can affect groundwater flow direction, lower solute transport times, and increase the potential for contamination through leaking or abandoned wells (Birdsell et al. 2015; McIntosh et al. 2019).

The Williston Basin is one of the largest oil and gas producing regions in North America. It makes up the southeastern section of the Western Canadian Sedimentary Basin and contains a total of ~95,000 oil and gas wells (IHS Markit 2020; North Dakota State Industrial Commission 2020). Water injection and disposal have been historically used in the Williston Basin for oil and gas production. However, there has been a substantial increase in production and, in turn, produced and injected water volumes in the last 30 years (Ferguson 2015). With the introduction of The Waterflood Development Program that incentivizes the conversion of producing wells into injection wells in Saskatchewan in 2019, it is expected that produced and injected water volumes will continue to increase in the Williston Basin. This continued growth in produced and injected water usage, coupled with a growing number of inactive or abandoned wells, has made it increasingly challenging to determine the effect of oil and gas production on the basin subsurface pressures, and the solute transport methods that lead to the potential contamination of surrounding aquifers.

1.1 Research Objectives

Many studies have examined the volumes of produced and injected water used for oil and gas production, and the effect of water injection and saltwater disposal on induced seismicity. However, there has been little discussion into the spatial distributions of these fluids and produced and injected volumes within the Williston Basin remain unclear. By examining the role of water usage in oil and gas production in the Williston Basin, this thesis aims to establish whether there have been significant enough changes in local fluid budgets or fluid budgets at the formation level to influence hydraulic gradients and associated reservoir pressures, even if injection volumes equal production volumes at the regional scale.

Specifically, the objectives of this thesis research are to:

1. Create a comprehensive fluid budget for each geologic formation within the study area, including total and monthly volumes.
2. Analyze representative formations to expand the understanding of production and injection rates over time, as well as current and historic production patterns.
3. Determine spatial fluid budget changes to identify regions of maximum fluid volume change.
4. Estimate potential pressure changes within selected formations using analytical models.

1.2 Thesis Structure

This thesis will cover and address all objectives throughout its six chapters. Chapter 2 provides an overview of the chosen study area and summarizes the relevant geology, hydrogeology, and geochemistry of the Williston Basin. Chapter 3 examines the use of water resources in the oil and gas industry and reviews the water usage of various production methods, as well as the potential effects of injection on formation pressures and the risk of groundwater contamination. Chapter 4 covers the methodology and data collection used in the study. Chapter 5 summarizes well volumes and the total basin fluid budget, as well as comparing the spatial variability of well densities and produced and injected water volumes for the entire basin and individual formations. Chapters 6 covers the modelling done to predict the changes in reservoir pressure influenced by the rates of production and injection. Chapter 7 contains the discussion that synthesizes and draws interpretations from empirical data and model predictions found in the previous chapters. Finally, a summary of the main conclusions and recommendations can be found in Chapter 8.

2. Study Area, Geology and Hydrogeology

2.1 Study Area

The project study area encompasses the majority of oil and gas wells present in southeastern Saskatchewan and western Manitoba. It covers an area of roughly 100,000 km^2, extending from longitude 106°W to 100°W and is bounded to the south by the 49th parallel, and to the north by latitude 51°N (Figure 2-1). The producing formations that the study area focuses on are part of the Williston Basin, which extends into regions of Saskatchewan, Manitoba, Montana, North Dakota, and South Dakota (Figure 2-1).

Hydrocarbon production on the Canadian side of the Williston Basin primarily occurs in the center of the basin and extends to the eastern margins. The study area contains 58,000 wells or roughly two-thirds of the total wells in the Williston Basin with over half of that number of wells being active in 2019. These wells are primarily production wells used for oil and gas production, along with a small mix of injection and saltwater disposal wells**.**

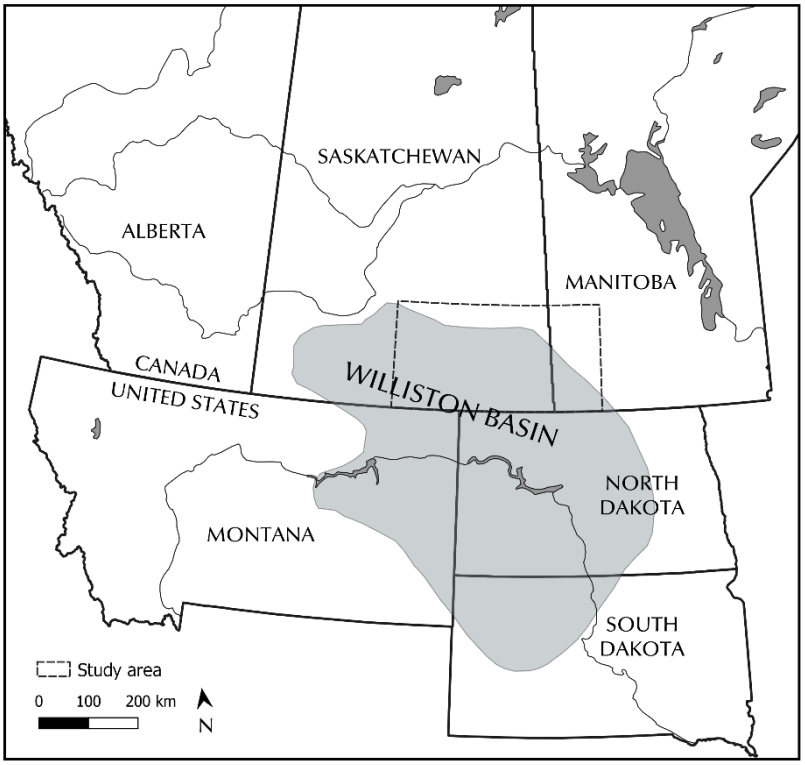

Figure 2-1: Location of the study area and the Williston Basin (Modified from Kuhn et al.,2011)

2.2 Geological Overview

The Williston Basin has undergone significant geologic assessment and mapping due to the presence of oil and gas (Gerhard et al. 1982; Peterson and MacCary 1987; Kent and Christopher 1994). Past studies have primarily focused on the geologic framework of the basin to determine potential source rocks, as well as the timing and formation of structures. Due to extensive oil and gas production, more than 95,000 wells have been completed in the Williston Basin, with more than four-fifths of the wells drilled on the Canadian side of the basin (North Dakota Mineral Resources 2019; IHS Markit 2020). However, studies of the basin's hydrogeology have been less frequent and have been conducted more recently (Bachu and Hitchon 1996; Hannon 1987; Palombi 2008).

2.3 Regional Geologic Setting

The Williston Basin is an intracratonic sedimentary basin made up of alternating layers of sandstone, carbonate, and shale dominated formations (Figure 2-3). It forms the southeastern extremity of the larger Western Canadian Sedimentary Basin and extends into parts of Saskatchewan, Manitoba, Montana, North Dakota, and South Dakota. The basin has an area of around 250,000 km² with topographic highs in Montana and lows in Manitoba and a maximum stratal thickness of 4900 m (Kent and Christopher 1994, 2008).

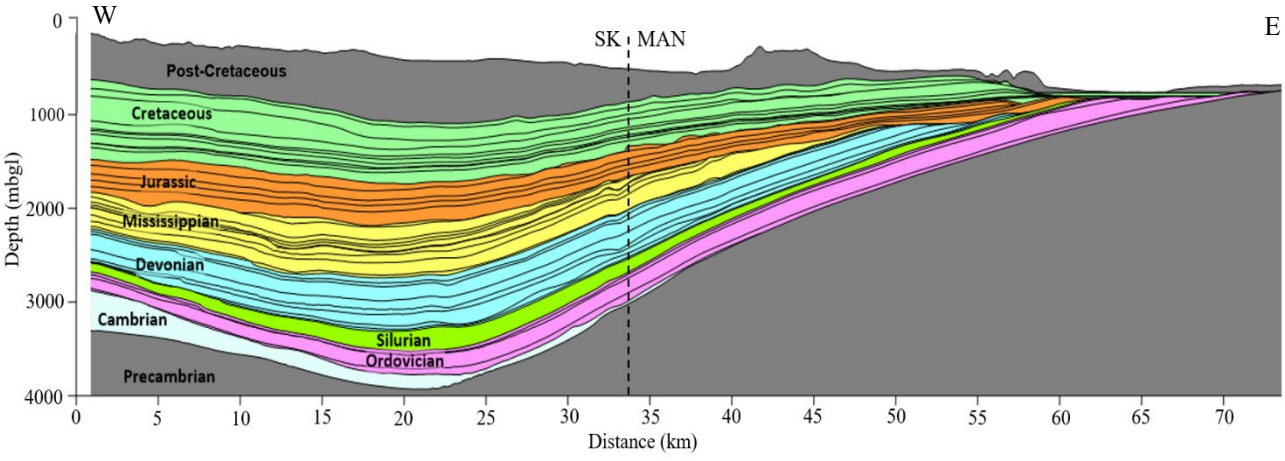

Figure 2-2: Cross section of the Williston Basin. Vertical Exaggeration = 5

The formation of the Williston Basin began during the Late Cambrian to Early Ordovician and lasted until the Late Cretaceous (Kent and Christopher 1994). The Williston Basin is structurally simple and contains a near-continuous sedimentary succession since the beginning of the Middle Cambrian until the late Cretaceous period. The basin's geologic characteristics can be attributed to its complex history of stratal thickening, thinning and truncation, caused by varying mechanisms of subsidence and controls on the basins geographic position (Ahern and Mrkvicka 1984; Kent and Christopher 2008).

The basin is bordered by a series of arches, domes, and uplifts. It is bordered to the west by the Sweetgrass Arch, which separates it from the Alberta basin, as well as the Black Hills uplift located further south (Kent and Christopher 1994). To the east, the basin is bordered by the Sioux uplift, and pinches out, forming the Manitoba Escarpment. These series of arches and uplifts cause the basin to plunge northeast from the southwestern outcrops reaching its maximum depth of 3,200 m near the Canada/US border then rises towards northwestern edge before outcropping in Manitoba.

2.4 Hydrogeology

Previous work in the Williston Basin has shown that the regional flow system is topographically driven. New meteoric waters are recharged in the southwest topographic highs of the Black Hills and flow towards the center of the basin before travelling northeast into the eastern erosional edge of the basin in Manitoba (Downey et al. 1987; Hannon 1987; Bachu and Hitchon 1996; Grasby et al. 2000; Weyer and Ellis 2013). Formation waters tend to flow laterally through aquifers with minimal cross formational flow due to a series of interspersed shale aquitards (Bachu and Hitchon 1996).

Both local and regional flow systems are present within the Williston Basin. Groundwater transit times in local flow systems range from <1000 to >30,000 years, while transit times in the regional flow systems are magnitudes longer (McMahon et al. 2011). The Williston Basin, along with numerous other sedimentary basins, also contain high density saline brines at depth. Due to the high density of these brines, the normal topographic drive is not sufficient to flush them from the basin (Palombi 2008; Ferguson et al. 2018). This lack of driving forces can trap brines within

the basin for long periods of time, brines in similarly structured sedimentary basins have been found to be tens of thousands to hundreds of millions of years old (Carpenter 1978; Hanor 1994; Schlegel et al. 2011; Darrah et al. 2015).

2.4.1 Hydrostratigraphic Units

Using the stratigraphic framework completed by previous studies, it is possible to categorize hydrostratigraphic units in the study area that represent aquifers, aquitards, or aquicludes. These divisions are defined at a local scale and comprise one or more geological units that exhibit similar properties, mainly permeability. Due to the disconnect between research occurring in Canada and the United States, the regional scale hydrostratigraphic system of the basin has yet to be fully developed. Instead, only major basin-scale systems based on rock lithologies and hydrogeological properties have been proposed. These major regional aquifers in the Williston Basin include the 1) Lower Paleozoic Aquifers and Aquitards 2) Mississippian Aquifers and Aquitards, and 3) Mesozoic Aquifers and Aquitards (Figure 2-4) (Palombi 2008).

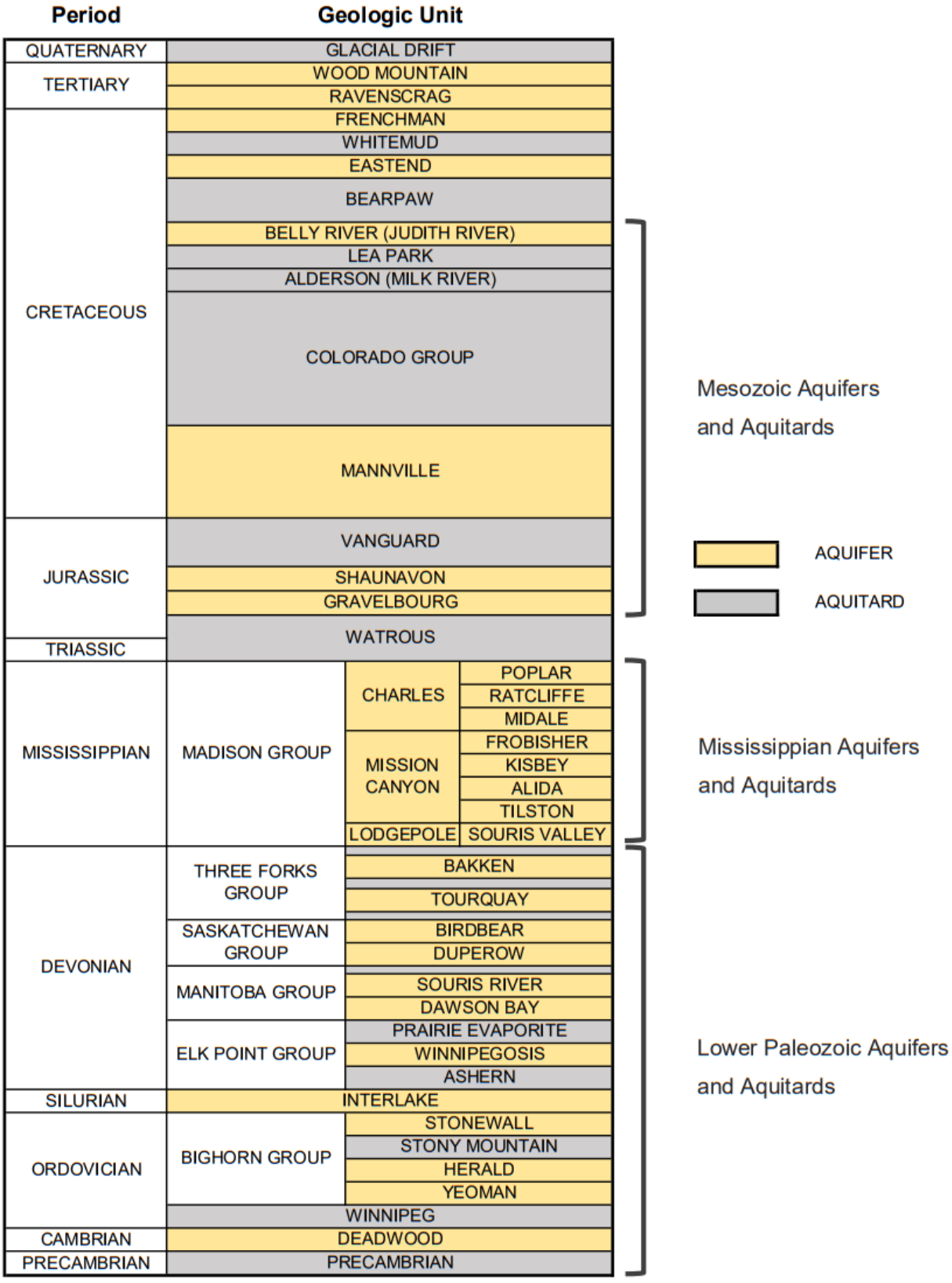

Figure 2-3: Williston Hydrostratigraphy (after Palombi, 2008)

Lower Paleozoic Aquifers and Aquitards

The Lower Paleozoic consists of eight separate aquifer groups split by confining aquitards. These aquifers include the: Cambro-Ordovician Aquifer, Yeoman Aquifer, Ordo-Silurian Aquifer, Winnipegosis Aquifer, Manitoba Aquifer, Duperow Aquifer, Birdbear Aquifer and, Bakken Aquifer.

The Cambro-Ordovician Aquifer is a basal clastic sequence composed of the Deadwood and the Winnipeg formations. The aquifer thickness varies throughout the basin, but at the centre of the basin, it forms one of the largest aquifers with an approximate total thickness of 300 m at the center of the basin (Palombi 2008). While hydraulic testing data is limited due to the lack of the wells, hydraulic conductivities between 1.0×10^{-6} to 1.1×10^{-3} m/s have been reported for this aquifer (Hutchence et al. 1986; Betcher et al. 1995; Ferguson et al. 2006). These aquifers are bound by the underlying Precambrian basement and by the overlying Icebox Member shales of the Winnipeg Aquitard. The Deadwood Formation has primarily been used for brine disposal from potash mining. In addition to saltwater disposal, there has been interest in developing this basal system for geothermal energy production due to its high temperature and heat flow rates or utilizing it as a large-scale carbon sequestration unit (Ferguson and Grasby 2014; Whittaker and Worth 2011).

The Yeoman Aquifer consists of the fossiliferous dolomite and dolomitized sandstone of the Yeoman and Red River formations. (Norford et al., 1994). It is bounded by the overlying Stony Mountain Aquitard, a uniform 22 m (maximum) thick formation made of mixed carbonates and shales (Palombi 2008).

The Ordo-Silurian Aquifer contains the Stonewall and Interlake formations. Together these formations form a homogenous dolomite sequence with thin sandy argillaceous markers (Bezys and Conley 1998). The Ordo-Silurian Aquifer is confined by the overlying Ashern Aquitard, a low permeability argillaceous and dolomitic shale formation (Palombi 2008). Both formations have the potential for petroleum production; however, within the study area, these formations are used primarily for saltwater disposal for potash mines. Despite the size of these carbonate aquifers and use for saltwater disposal, they are not the primary focus of this study due to their depth and separation from any fresh water-bearing aquifer.

The Winnipegosis Aquifer is a carbonate aquifer made up of limestone and dolomite. The aquifer exhibits heterogeneous permeability due to varying zones of high permeability fractures and inter-granular reefs, and low permeability zones made up of shale layers. The Winnipegosis Aquifer is confined by the overlying Prairie Evaporite Formation. The Prairie Evaporite primarily consists of halite with minor interbedded anhydrite and varies in thickness from 210 m to 0 m along the salt-dissolution edge of the formation (Nicolas 2015).

The Manitoba Aquifer includes the Dawson Bay and Souris River formations. The formations are both carbonates consisting of primarily limestone with some dolomite and anhydrite (Palombi 2008). It ranges in thickness from 115 m in Manitoba to 244 m in central Saskatchewan. It is overlain by the Souris River Aquitard, which consists of lower permeability calcareous shales and carbonates.

The Duperow Aquifer is a carbonate aquifer comprised of limestones and dolostones. It varies in thickness from 150 m in North Dakota to 215 m in Saskatchewan (Hoganson 1978). The Duperow Aquifer is overlain by the Seward Aquitard. A confining aquitard consisting of micro-crystalline limestone and capped by an anhydrite layer (Wilson 1967).

The Birdbear Aquifer consists of both lower and upper members of the Birdbear formation. The lower member is made up of limestones and dolostones, and the upper member consists of permeable dolostone, dolomitic limestone and anhydrite. It is confined by the overlying Three Forks Aquitard, which includes the Torquay and Big Valley formations. Both formations consist of low permeable carbonates and shales and have an average thickness between 45 to 50 m.

The Bakken Aquifer is an interbedded siltstone and sandstone aquifer that is sandwiched between two confining organic-rich shale aquitards. The Bakken Formation has a variable thickness across the basin with thicknesses between zero and a maximum of 47 m in North Dakota (Kreis et al, 2006). The Bakken aquifer is a significant oil-producing formation in Saskatchewan utilizing hydraulic fracturing since 2005.

Mississippian Aquifers and Aquitards

While the Mississippian Aquifer system is often classified as a single aquifer, it can be split into seven individual formations. These formations are often considered one aquifer due to difficulty in differentiating aquifers from the large amounts of chemistry and pressure data available for the

Mississippian aquifers, and due to the similarity of chemistry and hydraulic head measurements on the basinal-scale. Mississippian aquifers examined in this study include the Lodgepole, Tilston, Alida, Kisbey, Frobisher, Midale, Ratcliffe, and Poplar Beds. These aquifers are primarily permeable carbonate units. Hydraulic conductivities in the Mississippian aquifer system are estimated to be around 1.4×10^{-7} m/s (IHS Markit 2020).The Mississippian aquifers are host to large quantities of hydrocarbons, with nearly 50% of the wells in the study area producing from the Mississippian aquifers.

The Lodgepole Aquifer varies in lithology from mudstone to non-argillaceous carbonate rock and overlies the Bakken shale aquitard. It reaches thicknesses of up to 225 m in parts of North Dakota, and 70 m along its northeastern edge (Christopher and Yurkowski 2004).

The Tilston Beds overlies the Lodgepole aquifer and consists of argillaceous dolomicrite interlaminated with claystone. It ranges in thickness from 100 m in North Dakota to 0 m along the outcrop edge in the northeast (Christopher and Yurkowski 2004).

The Alida Beds is a carbonate unit that overlies the Tilston Aquifer. The thickness of the Alida Aquifer varies greatly across the basin, between 25 and 100 m depending on the region (Christopher and Yurkowski 2004).

The Kisbey Beds is a thin layer of siliciclastics between the underlying Alida Beds and overlying Frobisher Beds. The presence of siliciclastics within the Mississippian Group is unique to the Kisbey Beds. The stratigraphic thickness of the Kisbey Beds ranges between 1 and 10 m, with some regions northeast of Estevan reaching thicknesses of 34 m (Christopher and Yurkowski 2004).

The Frobisher Beds are primarily carbonate rocks, ranging from lime mudstones to dolostones. The carbonate layer is overlain by the Frobisher Evaporite, an isolated anhydrite layer. The thickness of the Frobisher Beds ranges from 5 to 105 m, reaching its thickest along the northeastern edge before pinching out (Christopher and Yurkowski 2004).

The Midale Beds consists of two varying carbonate units, the Marly and Vuggy. The upper Marly unit is a variably fractured dolostone layer with argillaceous laminations. The lower Vuggy layer is primarily limestone with mineralized vugs. In some areas these two units can be overlain by a low permeability third unit; the Midale Evaporite (Pendrigh 2005). The total

thickness of the Midale Aquifer ranges from 22 m in along the U.S.-Canada border to 0 m along the edge of the formation to the northeast (TGI Williston Basin Working Group 2008).

The Ratcliffe Beds overlies the Midale Beds and is dominantly lime mudstones and wackestones. Thickness ranges between 6 to 21 m, with maximum thickness occurring in eastern Montana (Christopher and Yurkowski 2004).

The Poplar Beds overlies the Ratcliffe Beds and is the uppermost unit in the Mississippian Group. Its lithology consists of alternating lime mudstones, dolomicrites, dolostones and anhydrite. It has a max stratigraphic thickness of 260 m in Montana and North Dakota, thinning to 0 m along its northern border. It is the thickest formation in the Mississippian group of aquifers (Christopher and Yurkowski 2004).

Mesozoic Aquifers and Aquitards

The Jurassic Aquifer includes the Gravelbourg and Shaunavon formations. Both formations are primarily carbonate formations that together range in thickness from 80 to 100 m. They are confined by the overlying Vangaurd Aquitard, a 100 m thick shale formation.

The Mannville Aquifer is made up of interbedded sandstones and shales and is the highest permeability aquifer within the Mesozoic group of aquifers. The permeability is estimated to be as high as 10^{-8} m^2 (Khan and Rostron 2005), and it has a thickness of up to a maximum of 150 m. The hydraulic conductivity is reported to be between 7×10^{-6} to 7×10^{-7} m/s (MDH Engineered Solutions 2011). The Mannville Aquifer is confined by the Colorado-Lea Park Aquitard. This aquitard is comprised of a 300 m thick layer of dark low permeability shales. The Mannville has historically been a major source of water for use in oil and gas production but has primarily been used for saltwater disposal since the 1990s.

The Judith River Aquifer is a clastic aquifer comprised of primarily sandstones and siltstones. The formation can exceed 360 m in thickness in Alberta but becomes thinner in Saskatchewan (Christopher 2003). It is confined by the Bearpaw Aquitard. The Bearpaw Aquitard is a thick shale aquitard like that Colorado-Lea Park Aquitard, with thicknesses exceeding 425 m in southern Saskatchewan (Maathuis 2008).

2.4.2 Geochemistry

Oil and gas production within the basin has led to the development of a substantial database of formation water data. While the samples collected do not necessarily allow for a detailed analysis of each formation, they can be used to create a regional assessment of total dissolved solids and bulk geochemistry values. From these databases, we can see that formation waters in the Williston Basin are dominantly Na–Cl waters and range widely from 2,000 to 350,000 mg/L total dissolved solids (TDS) (Grasby et al. 2000). TDS values show little trend in relation to depth but jump significantly below the Prairie Evaporite (Figure 2-5). Past studies of fluid chemistry and isotopes have suggested this increase in TDS is due to the presence of a residual paleo evaporated seawater-derived brine (Hitchon et al. 1971; Spencer 1987; Connolly et al. 1990; Simpson et al. 1987; Hendry et al. 2013). This mass of brine remains at depth as the topographic flow is not enough to drive the flow of this dense fluid out of the basin (Palombi and Rostron 2006; Ferguson et al. 2018).

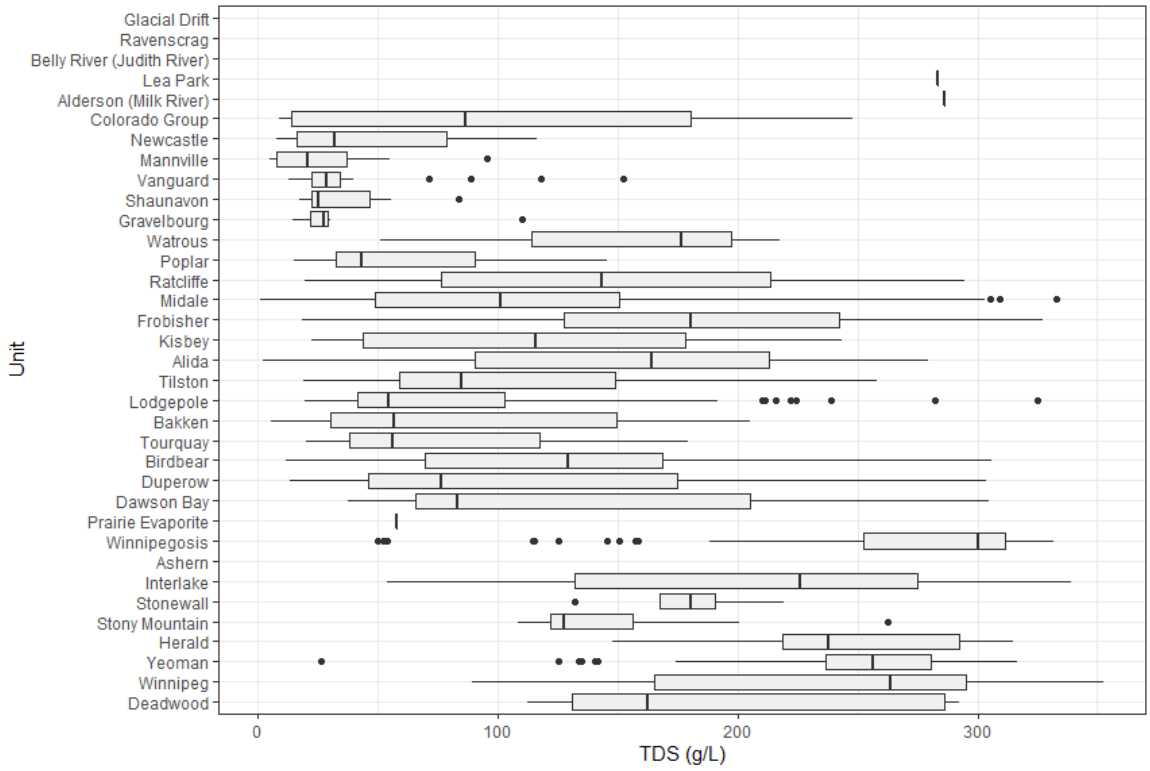

Figure 2-4: Total Dissolved Solids for each formation descending with depth. The boxes represent the first and third quartiles (25th and 75th percentiles), the line represents the median, the whiskers represent the minimum and maximum of the data (1.5 * IQR), and a circle indicates an outlier.

3. Oil and Gas Production and Impacts on Water Resources

Oil and gas have been produced in Saskatchewan since the first commercial crude oil discovery was made in the province in 1944. Since then, Saskatchewan has become Canada's second-largest oil and gas producer (Alberta Energy 2015). Despite a lengthy history of oil and gas production in Saskatchewan, there are still large knowledge gaps on the effects of oil and gas production on subsurface hydrogeology.

3.1 Production Methods in the Williston Basin

The first commercial gas well in the Williston Basin was established in 1913 in Montana, and the first commercial oil well was established in 1951 in North Dakota (Anna et al. 2010). This marked the beginning of consistent oil and gas production in the US, with Canada to follow shortly after with several wells drilled in 1953 (IHS Markit 2020). Since then, oil and gas production has increased as new fields are discovered, and new technologies are developed.

As oil and gas production has progressed in the Williston Basin it has utilized primary, secondary, and tertiary recovery. Primary recovery methods utilize the natural drive of pressured reservoirs or artificial lift produced by pumping devices to bring hydrocarbons to the surface. Secondary recovery methods use the injection of water or gas to either displace the oil from pore spaces or to maintain reservoir pressure. Tertiary recovery or enhanced oil recovery (EOR) methods use the injection of water or gas to alter the properties of the reservoir making it easier to produce, this includes methods such as thermal recovery, CO_2 injection, or chemical injection.

Between the 1950s and 1990s, oil and gas production was completed solely through vertically drilled wells in conventional plays using primary and secondary recovery methods. During this time, oil production underwent several cycles, a peak in the mid-1960s before a dip in the 1980s, then a steady rise in production until the mid-2010s. This increase in production after the 1980s can be attributed to the expansion into unconventional oil reserves that relied on the development and utilization of horizontal drilling. Horizontal drilling provided more contact with the reservoir reducing the number of wells required and immensely increased well productivity. By 2008 oil producers in the Williston Basin were drilling twice as many horizontal wells than vertical wells, with that number reaching 13 times more in 2016.

In 2005, the use of high volume hydraulic fracturing (HVHF) in North America rose greatly due to high natural gas and oil prices, the availability of lease positions, and the economical application of new drilling and stimulation technologies (Soeder 2018). The newly accessible unconventional reserves were largely shale plays containing a mix of oil and natural gas. This included the Canadian-U.S. shared Bakken oil-bearing shale (Soeder 2018). The use of HVHF has been a controversial topic in academic literature and public opinion since its inception, creating debates on water quality, environmental impacts and fugitive methane in overlying aquifers. Despite the discussions, HVHF only represents <5% of contamination cases in the US (Brantley et al. 2014; Llewellyn et al. 2015; Sherwood et al. 2016).

3.2 Water Use in the Oil and Gas Industry

Conventional and unconventional oil and gas plays can vary drastically in both the volumes of water used in production, and volumes of water produced per unit of oil. As the number of wells in unconventional plays grow and new plays begin to be produced, it is important to assess the role of water in oil and gas production. Several studies have already compared the volume of water used for conventional versus unconventional oil. Conventional wells in the Permian Basin had water-oil ratios (WORs) of 14, which is significantly more than the WOR of 2.6 associated with unconventional wells (Scanlon et al., 2019). In the Bakken WORs were lower, 5 for conventional wells and 0.7 for unconventional wells (Scanlon et al. 2019). Oil recovery methods in conventional plays had been found to have WORs of 0.1−5, while unconventional plays utilizing HVHF were 0.2−1.4 (Scanlon et al. 2014). Primary recovery methods are relatively less water demanding having a WOR of ~0.2. Secondary recovery methods that involve the injection of water or gas to displace the oil, can be as high as WOR: ~8.6 over the lifespan of the well (Scanlon et al. 2014). Studies have shown that this secondary recovery can account for 80% of all water used for oil recovery (Wu et al. 2009), and has been shown to reach up to 90% in places such as the Permian Basin (Scanlon et al. 2017)

Studies have shown that HVHF methods use large quantities of water. In 2014 it was estimated that wells in the US used a median of 15,275 to 19,425 m^3, of fracturing water per well. This is up significantly from an estimated 670 m^3 per well in 2000. Conventional wells in the Midland Basin comparatively used an estimated 9,450 to 17,715 m^3 of water over the well's lifespan. (Gallegos et al. 2016).

Between 2005 and 2015, the total produced water in the Permian Basin was 7.0 x 10^9 m^3. Conventional wells accounted for 90% of the produced water, with unconventional wells producing the remaining amount. During the same time, injected or disposed of water was roughly 16% higher than produced waters (Scanlon et al. 2017).

3.3 Effect on Formation Pressures

The effects of injection on reservoir pressures are often overlooked compared to those induced by HVHF, but they can impose their own variety of complications within a reservoir. The over-pressuring of deep aquifers may drive injected waters into neighbouring potable water-bearing formations, damage well integrity (Kiran et al. 2017), and lead to induced seismicity in some cases (Rubinstein et al. 2015). Due to the lengthy time of increased pressure from water or gas injection in secondary production methods (up to 50 years), it is hypothesized that this could lead to more issues than the higher pressure but shorter period of HVHF (McIntosh and Ferguson 2019).

The increased reservoir pressure due to water or gas injection in secondary production methods can lead to contamination of neighbouring fresh water-bearing formations due to subsurface leaks from imperfectly cemented oil and gas wells or decaying legacy wells. The increased pressure can reverse the hydraulic gradient causing fluid to flow up wells and can increase the distance of solute transport. Even though the increased pressure of sustained water and gas injection is less than HVHF, the duration of injection can cause the solute distance to increase 100 fold (McIntosh and Ferguson, 2019). This can happen in both naturally-present faults and in compromised wells.

4. Methodology

4.1 Data Collection

To evaluate whether the fluid flow has been rearranged at the basin scale due to production and injection activities, a database of 57,624 oil and gas wells was created for the entire study area. This database was created by utilizing well data provided through AccuMap (IHS Markit 2020), a data management and analysis software produced by IHS Markit. Supplementary data was also referenced from the Integrated Resource Information System (IRIS) (www.saskatchewan.ca/iris), an online database managed by the Government of Saskatchewan's Ministry of Energy and Resources.

AccuMap compiles and digitizes private and governmental oil and gas data from across the WCSB into one integrated dataset. Querying this dataset by formation, area, time, etc. provides a way to create a meaningful collection of data specific to the study area. The primary data collected from AccuMap for use in this study included; well locations, producing zones, well types, well modes, cumulative and monthly production and injection volumes, well operation dates, and fluid chemistry values.

IRIS acts as a portal for industry members to submit applications, permits, and required data applying to oil and gas processes. It stores all submitted data and reports, making them available to search and view. IRIS was used in this study for individual well specific data, including original reports and data records.

4.2 Data Analysis

To improve the quality and useability of the study area well dataset, the numerous classifications for a single producing zone provided by drilling logs were sorted and grouped into a single formation classification based on stratigraphic columns created by the Saskatchewan Ministry of Economy. This reduced the number from 147 formation classifications provided by drilling logs to 36 classifications used in the dataset. In cases where multiple formations were provided in the producing zone classification, the formation list first was used. Formations that exist under different names in Manitoba were also reclassified with the respective Saskatchewan specific formation name.

To fully understand the spatial complexity and spacing of oil and gas wells, maps were created using Geographic Information System (GIS) software. Two sets of maps were created, showing the distribution of wells and the distribution of fluid volume changes, highlighting areas with high densities of wells and regional variations in production and injection volumes. To do this, the study area was broken down into a grid of 5 km x 5 km cells. The number of wells present within each cell was then calculated, and production and injection volumes for every well in the cell were combined. To make it easier to comprehend volumes of these fluids, they are presented as a total millimetre change per square metre area.

4.3 Background Flow Rates

To quantify the volume of fluid being injected into reservoirs, the yearly injection rate was compared to the yearly background flow rate for each formation. The background flow rate is the annual volume of new water entering a grid cell naturally. The flow rates occurring in each formation were estimated using Darcy's Law for fluid flow through a porous media:

$$Q = -kA \cdot \frac{\Delta h}{L} \tag{4.1}$$

Where Q (m^3/s) is the volumetric flow rate, k is the hydraulic conductivity of the reservoir (m/s), A (m^2) is the cross-sectional area of the reservoir, Δh (m) is the change in pressure head, and L (m) is the length. Reservoir parameters are consistent with those used to calculate reservoir pressure changes.

The area was calculated by multiplying the width of the modelled cell by the total thickness of the reservoir. Hydraulic gradients ($\frac{\Delta h}{L}$) were calculated from hydraulic head maps published by Palombi in 2008, and are based on earlier, pre-development data. Background flow rates were then compared to the anthropogenic flow rate caused by oil and gas production. The anthropogenic flow rate is the annual volume of excess water being introduced into a grid cell due to oil and gas production.

4.4 Modelling Reservoir Pressure Changes

The response in reservoir pressure due to the influence of injection and producing wells was modelled analytically using Aqtesolv (HydroSOLVE Inc. 2016) and Surfer® (Golden Software LLC 2020). Aqtesolv is commonly used to simulate changes in the hydraulic head due to the influence of surrounding pumping wells. Since Aqtesolv is only capable of simulating pumping rates, two different models were created for injection and production rates, and then superimposed over each other using Surfer.

For each model, the monthly injection and production rates for each well were obtained using AccuMap and were converted into daily rates input into the model. An average total aquifer thickness for each model was based on reported thicknesses provided by well logs in the model area.

For the reservoir pressure models of the Mannville Group and the Midale Member it was assumed that each aquifer is a uniform thickness, is isotropic, the wells are fully penetrating, and fluid flow is single phase. While it is clear that the formational fluid will not be a single-phase due to the presence of oil and gas, it is assumed that the much smaller volume of oil will not have a significant impact on the overall formational pressures created by the injection of waters. Horizontal wells have also been treated as producing or injecting from a single point instead of along the entire length of the horizontal screen. While modelling horizontal wells is possible, the computational time needed to calculate pressures was significantly higher, with only minimal variations in modelled pressure changes. Differences in modelled pressure changes between horizontal and vertical wells varied by 20% at the wellhead, 5% at 150 meters, with pressures being identical past 500m. Visualizations of modelled pressure differences caused by using vertical wells instead of horizontal wells can be found in Figure A-1.

The hydraulic response in the reservoir caused by the wells was estimated in Aqtesolv using the Theis equation as follows:

$$s(t) = \frac{Q}{4\pi T}\int_{u}^{\infty}\frac{e^{-y}}{y}\,dy \tag{4.2}$$

where

$$u = \frac{r^2 S}{4Tt} \tag{4.3}$$

s(t) (m) is the drawdown over time, Q (m^3/s) is the well pumping or injection rate, r (m) is the radial distance from the well, S (dimensionless) is the storativity of the reservoir, and T (m^2/s) is the transmissivity of the reservoir. The Theis equation assumes a fully penetrating well pumping at a constant rate from a homogenous, isotropic, nonleaky confined aquifer of infinite extent. Due to the nature of deposition of the Williston Basin, most formations are confined units of uniform thickness with relatively homogeneous lithologies and extend across the entire basin, meeting the assumptions required by the Theis equation. The only assumption of the Theis equation that is not met is the nonleaky boundaries, as there is often cross-formational flow between the units. Additionally, while the fluids present in the formation have a much lower density than freshwater, it was deemed acceptable to use a head-based formulation as fluid density is considered uniform across the aquifer and flow is primarily horizontal in this analysis.

To calculate the hydraulic response by using the Theis equation, it was necessary first to determine the required reservoir hydraulic properties. Reservoir thickness was obtained from drilling records provided by IRIS of a well within the modelled area. A representative value of permeability and porosity data was found in previous literature and calculated from data provided by AccuMap (Beliveau 1989; IHS Markit 2020; MDH Engineered Solutions 2011).

The storativity of an aquifer is the volume of water that is released from storage per unit surface area of the aquifer per decline in the hydraulic head. Within a confined aquifer, storativity can be calculated with the following equation:

$$S = S_s b \tag{4.4}$$

Where S (dimensionless) is storativity, S_s (m^{-1}) is the specific storage, and b (m) is the thickness.

The specific storage (S_s) (m^{-1}) is the volume of water removed from a unit volume of a confined aquifer per unit drop in hydraulic head. It is related to the compressibilities of the aquifer and the fluid.

$$S_s = \rho_w g(\alpha + n\beta) \tag{4.5}$$

Where ρ_w (kg/m^3) is the density of the reservoir fluid, and g (9.81 m/s^2) is the gravitational acceleration constant, α is the aquifer compressibility (Pa^{-1}), n (dimensionless) is the aquifer porosity, and β is the compressibility of the reservoir water. The aquifer compressibility was

based on values presented in related literature on the characteristics of target formations (Beliveau 1989).

Transmissivity is the rate of flow through a unit width of an aquifer. Transmissivity can be calculated by converting permeability data into a hydraulic conductivity using an equation (4.6) developed by Muskat (1937) that relates Darcy's permeability and the weight of a fluid:

$$k = K\frac{\mu}{\rho_w g} \tag{4.6}$$

where k (m^2) is the permeability, K (m/s) is the hydraulic conductivity, μ (Pa·s) is the dynamic viscosity of the fluid, ρ_w (kg/m^3) is the density of the fluid, and g (9.81 m/s^2) is the gravitational acceleration constant. Once a hydraulic conductivity has been calculated, it is possible to calculate transmissivity using the following equation:

$$T = Kb \tag{4.7}$$

Where T (m^2/s) is the transmissivity of the reservoir, K (m/s) is the hydraulic conductivity of the reservoir, and b (m) is the thickness.

Once all the reservoir parameters were characterized, and input into the Aqtesolv, two models were created to simulate the change in the hydraulic head. One model used well production rates and one that used well injection rates. Individual contour maps of hydraulic head changes for each production and injection model were then created using Surfer®. To combine the production and injection rate models into a single contour surface the values of the production contour were multiplied by -1. The contour surfaces were then summed at each grid point using the Grid Math function in Surfer®. This created a contour of the difference in hydraulic head changes due to production and injection wells. To convert the change in the hydraulic head ($\Delta\psi$) to simulated reservoir pressure (ΔP)(Pa) changes, the following equation was used:

$$\Delta P = \Delta\psi g\rho_w \tag{4.8}$$

where g (9.81 m/s^2) is the gravitational acceleration constant and ρ_w (kg/m^3) is the density of the reservoir fluid. This function was also performed using the Grid Math function in Surfer®.

5. Temporal and Spatial Distribution of Wells and Produced and Injected Fluids

The mix of conventional and unconventional reservoirs in the Williston Basin and large quantities of produced and injected water make it difficult to understand whether the fluid flow has been rearranged at the basin scale due to oil and gas production. To better explain the role of oil and gas in basin fluid budgets and fluid flow, this study analyzed the volumes of produced and injected water, and number of wells within the study area. In addition, the spatial distributions of production and injection wells, and produced and injected water was compared across the entire basin and multiple formations.

5.1 Well Inventory

The study area covers multiple overlapping oil and gas pools and plays. These pools and plays exist in formations of differing lithologies, which require different production methods. Within the study area, there are more than 57,000 total wells, with over half of that number being active in 2019. This includes 28,100 active wells, 2,890 injection and disposal wells, and 15,339 abandoned wells. A total breakdown of well modes for the study area can be found in the Appendix (Table 3). Of the 36 recognized formations within the Williston Basin, a total of 18 formations are considered to be producing. Four formations contain the majority of the wells, led by the Midale with 8,428, the Bakken with 6,718, the Frobisher with 6,763, and the Tilston with 2,703 wells.

While historically conventional vertical wells were common, the use of HVHF and horizontal wells has become prevalent, beginning in 2005, as the rapid adoption of new technologies made it possible to produce from once uneconomical formations (Fig. 5-1). Within the study area there are 28,651 vertical wells, 22,214 horizontal wells, and 1,153 directional/deviated (dir/dev) wells (Figure 5-1). Due to current trends, it is expected that horizontal wells will soon outnumber vertical wells.

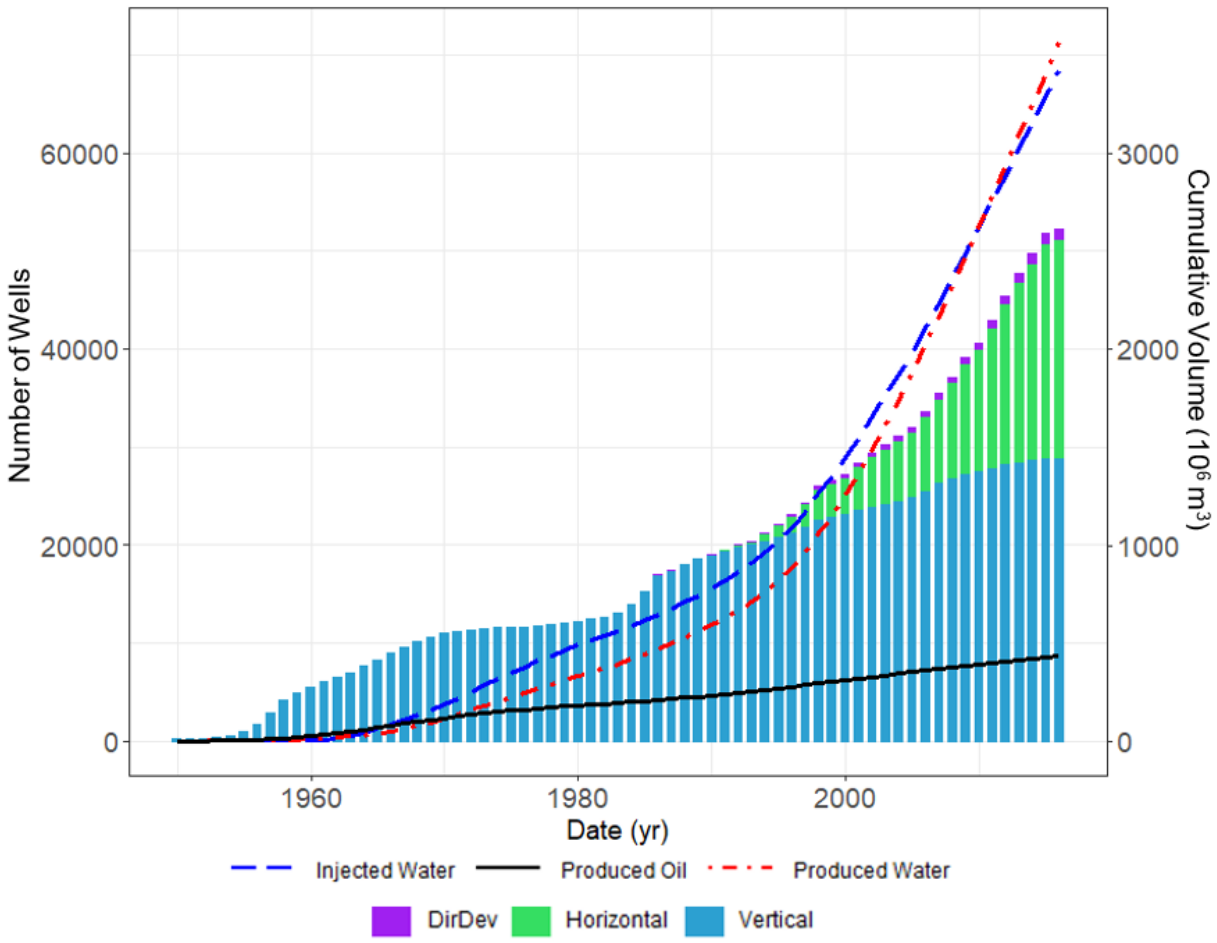

Figure 5-1: Type of well compared to the volume of fluid within the study area.

5.2 Total Fluid Budget

To create a comprehensive fluid budget of the study area and improve the understanding of formational volumes of produced and injected water, a database of total production volumes for each well, as well as monthly production volumes was created. This provided the ability to analyze trends in large-scale oil and gas fields to improve the understanding of the cumulative volumes represented. While a percentage of the water produced from a formation may have come from a connected overlying or underlying formation, all volumes are assumed to have originated from the single formation for ease of analysis.

Over the last 60 years within the study area, a total of 540 x 10^6 m^3 of oil, and 51 x 10^9 standard m^3 of gas have been produced, the quantity of produced water is nearly ten times this amount. In total, nearly 4.6 x 10^9 m^3 of water have been produced from within the study area. In turn,

another 5.5 x 10^9 m^3 of water was injected back into formations for use in water flooding or as saltwater disposal. In addition to these values, there are much smaller quantities of produced CO_2 and injected oil, gas, and CO_2.

When fluid volumes are dissected into individual formations, it highlights the grouping of formations that contain the most fluid movement. As seen in Figure 5-2, the bulk of fluid movement occurs within the Mannville Group, the Madison Group (Poplar Ratcliffe, Midale, Frobisher, Kisbey, Alida, Tilston and Lodgepole) and the Bakken Formation. Considerable quantities of water are also being injected into the Interlake, Stonewall, and Deadwood formations via saltwater disposal for potash mines.

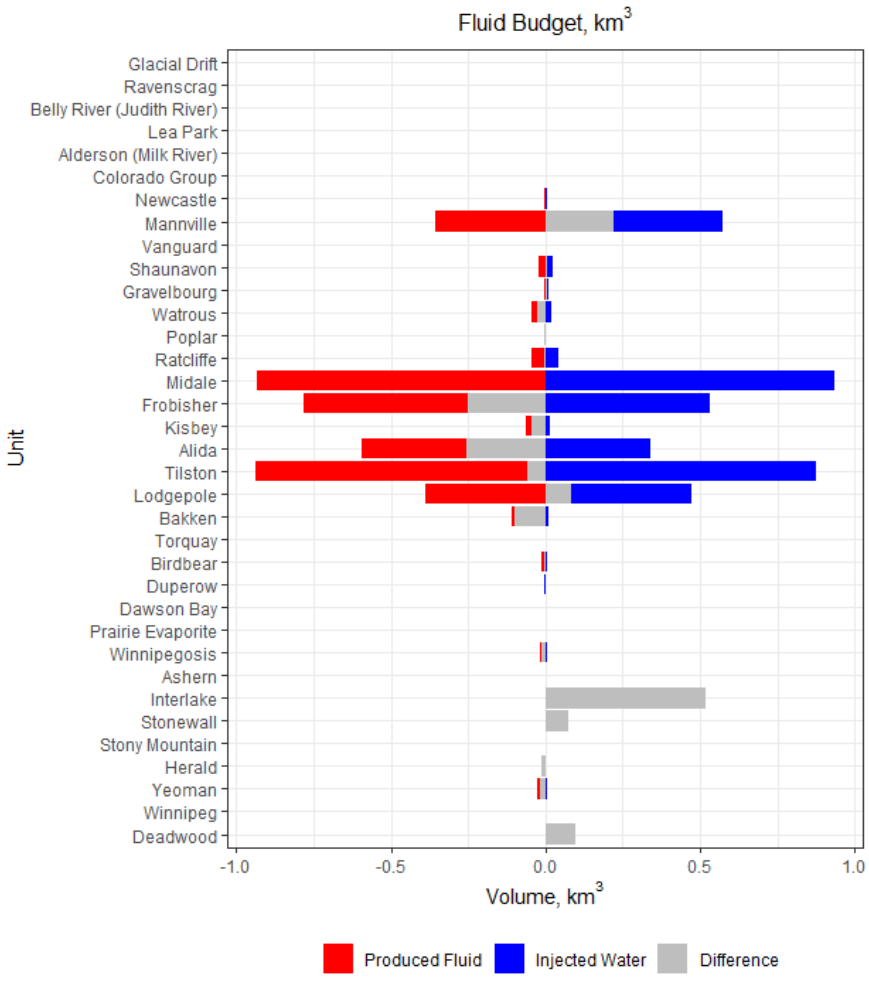

Figure 5-2: Difference in produced fluid (red) and injected water (blue) within formations in the Williston Basin. The difference (grey) represents the difference in produced fluid and injected water. Only formations with wells completions were included, and any formations missing from the figure are assumed to have unchanged volumes.

The study identified the Mannville Group, the Midale Member, and the Bakken Formation as key units for analyzing fluid movement patterns. The Mannville Group was selected due to having the largest surplus of injected fluid volume, excluding formations used for potash saltwater disposal. The Midale Member (of the Madison Group) was selected as it had the largest cumulative volume of produced and injected fluids while exhibiting almost no change of fluid volume within the formation. Due to the similar lithologies of members within the Madison group, it can be assumed that the observed changes in fluid budgets and associated reservoir pressures within the Midale Member, can also occur to some extent in other formations within the Madison Group. The Bakken Formation was selected due to its relatively recent production history and its use of HVHF as a primary extraction method.

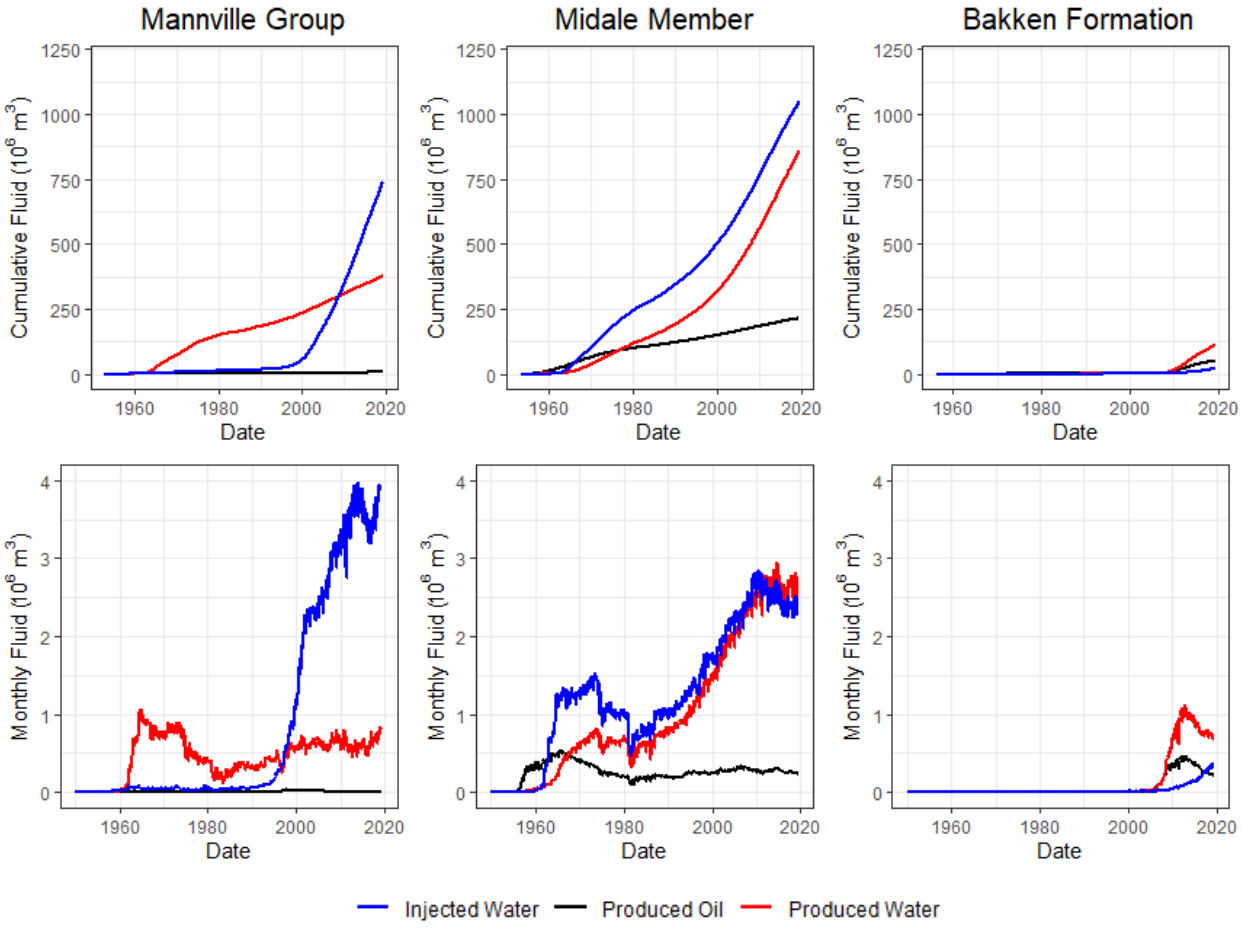

Figure 5-3: Cumulative fluid volumes (106 m3) and Monthly fluid rates (106 m3) for the Mannville Group, Midale Member, and Bakken Formation. The Mannville Group has produced the most water and has the lowest monthly injection rate. The Midale Member has similar production and injection rates, due to primarily utilizing waterflooding for production. The Bakken Formation uses the lowest volume of water and the most recently produced unit.

As of mid-2019, the Mannville Group has produced a total of 6.1 x 10^6 m^3 of oil, 376 x 10^6 m^3 of water and a negligible volume of gas. Additionally, there have been 726 x 10^6 m^3 of produced water injected into the formation, creating a surplus of 344 million m^3 of fluid (Figure 5-3). Despite the widespread use of the Mannville Group as a disposal reservoir not beginning until the late 1990s, it only took a short period of time for injected water volumes to surpass monthly produced water rates. Within ten years of injecting, the cumulative volume of injected water began to exceed the volume of produced water. The volume of produced water from the Mannville has stayed relatively constant over the active lifetime of the formation.

The Midale Member has produced a total of 215 x 10^6 m^3 of oil, 860 x 10^6 n m^3 of water and 26 x 10^9 m^3 of gas. Additionally, there have been 1.05 x 10^9 m^3 of water injected, resulting in a loss of 25 million m^3 of fluid within the formation (Figure 5-3). Oil production rates in the Midale have remained relatively stable since the beginning of production in the 1950s. While there was significantly more water injected than produced between the 1960s to 1980s, after this period, these rates become comparable and follow a similar trend. The flattening of injection and production rates in the Midale that occurs around 2010, correlates to a similar timeframe where production in the Bakken began.

The Bakken Formation has produced a total of 50 x 10^6 m^3 of oil, 110 x 10^6 m^3 of water and 6.4 x 10^9 m^3 of gas. Additionally, there have been 22 x 10^6 m^3 of produced water injected into the formation, resulting in a loss of 140 x 10^6 m^3 of fluid within the formation (Figure 5-3). The volumes of produced and injected water within the Bakken are significantly lower than those found in the Mannville and the Midale, however, produced oil rates are comparable to rates found in conventional formations like the Midale. This difference in produced water volumes between the Midale Member and the Bakken Formation while producing a similar volume of oil can be attributed to the type of production methods. Conventional wells typically produce ~13 times more water than oil (water to oil ratio, WOR) when compared to unconventional oil wells (Scanlon et al. 2014). The Midale Member, which primarily utilizes waterflooding methods for oil production, exhibits a WOR of ~10, while the Bakken formation has a WOR of ~3. Formations with similar hydrogeologic properties to the Midale have even higher WORs, reaching as high as ~40 in the Mission Canyon Group.

5.3 Spatial Variability

5.3.1 Well Densities

Examining the location of wells and well densities can provide greater insights into regions that are more likely to experience effects due to oil and gas production. While considering all wells within the study area is important to highlight regions with the highest density of wells, it is also important to examine well densities on an individual formation basis. Currently there are ~58,000 wells within the study area. Well fields focused on higher densities in the small region that stretches from the centre of the study area along the Canada–US border to the eastern edge of the Williston Basin. Wells can be found sporadically across the rest of southern Saskatchewan up to the western border, where well densities sharply increase (Figure 5-4).

Wells within the Mannville Group are fairly spread out when compared to well densities in other formations (Figure 5-4). The average well density per cell across the study area is only 2.8 wells per 25 km^2, while the maximum density is 147 wells per 25 km^2. The sparseness of wells can be attributed to the fact that 40% of these wells are disposal wells. These disposal wells often service many surrounding production wells requiring a lower volume of wells in larger spacing.

Wells in the Midale Member are tightly grouped within the middle of the study area and extend toward the Canada–US border (Figure 5-4). The Midale Member has the highest average density of wells of the formations, at 31.1 wells per 25 km^2, as well as the highest number of wells in one cell at 299 wells. This high density of wells is due to the use of water flooding within the formation. These water flooding patterns extend across the entire oil and gas play, causing the well density map to appear solid with few gaps due to lack of wells.

The wells in the Bakken Formation primarily split into three main groupings, one along the bottom of the study area, one in the center, and one towards the eastern edge extending into Manitoba (Figure 5-4). The average well density in the Bakken is 17.3 wells per 25 km^2, with a maximum of 191 wells. Wells are primarily focused in the center of each one of these groupings, with the density of wells decreasing outwards.

5.3.2 Fluid Distribution

To compare the fluid volume distribution across the study area, injected and produced water volumes (m^3) were divided by the area of the 5 x 5 km cells (25 km^2) to present the volume change in mm. While injected water will not necessarily stay within the confines of the cell it is injected in, this method helps highlight areas of above average amounts of injected or produced fluids. In study area (Figure 5-5), the total maximum increase in fluid volume per 25 km^2 cell was 8,995 mm. The maximum decrease in fluid volume was 3,315 mm, and the average change across all cells was 3.9 mm. The Mannville Group had a maximum increase in fluid volume of 1,026 mm, and a maximum decrease of 3,851 mm. The average change across all cells in the Mannville Group was 3.4 mm. The Midale Member had a maximum increase in fluid volume of 497 mm, and a maximum decrease of 529 mm. The average change across all cells in the Midale Member was -0.3 mm. The Bakken Formation had a maximum increase in fluid volume of 32 mm, and a maximum decrease of 126 mm. The average change across all cells in the Bakken Formation was -1.4 mm.

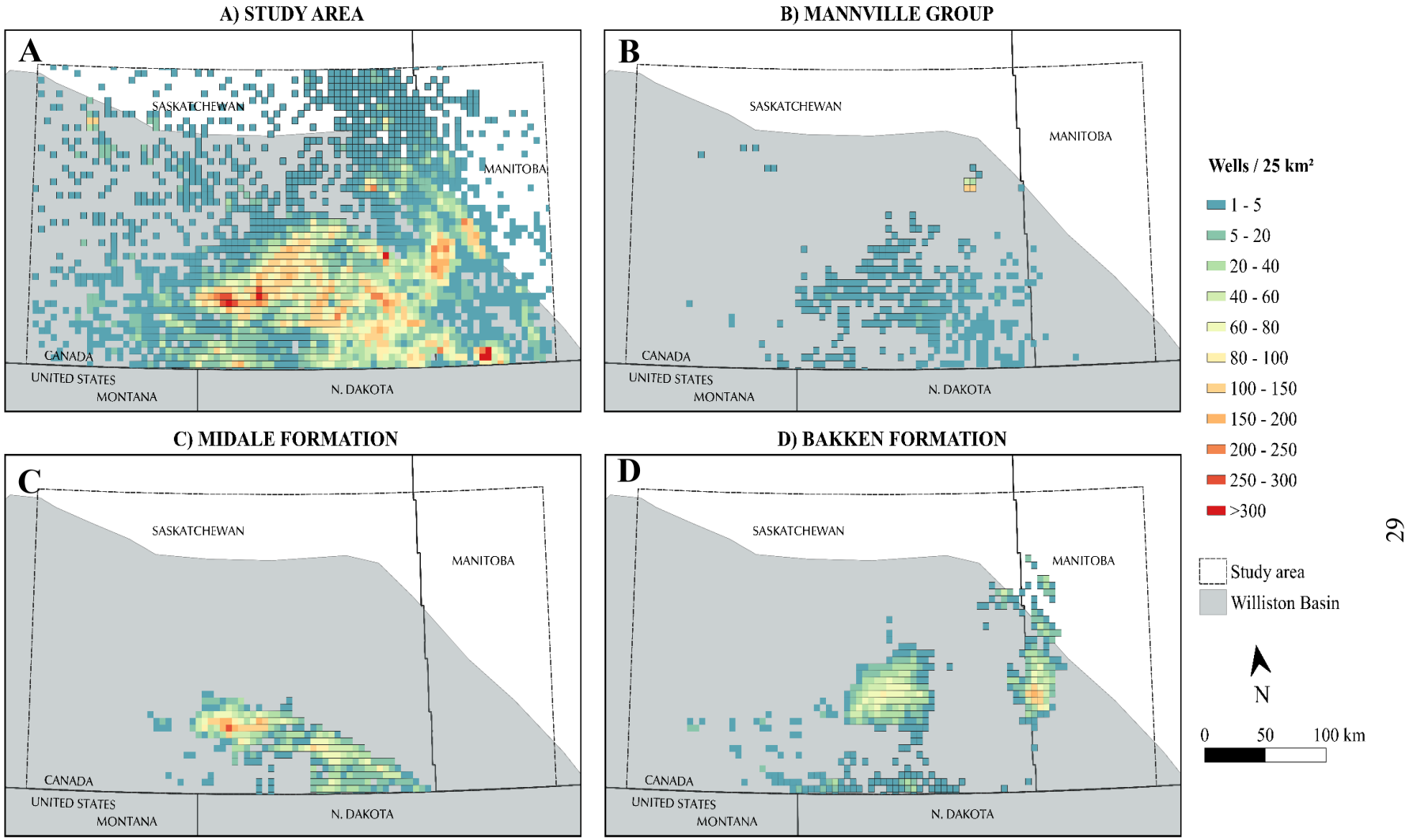

Figure 5-4: Well Counts per 25 km^2. A) This covers every well within the study area regardless of formation or group, this highlights surface regions with high densities of wells (avg 26.7 wells/25 km^2). B) Mannville Group wells are commonly spread out much more than wells in other formations (avg 2.8 wells/25 km^2), this is due to the formation being primarily used by disposal wells that service many other wells. C) Wells in the Midale are tightly grouped when compared to other formations (avg 31.1 wells/25 km^2), that make up a majority of production within the centre of the study area. D) Bakken Formation wells are split into three groups, with the easternmost group having the highest density of wells (avg 17.3 wells/25 km^2).

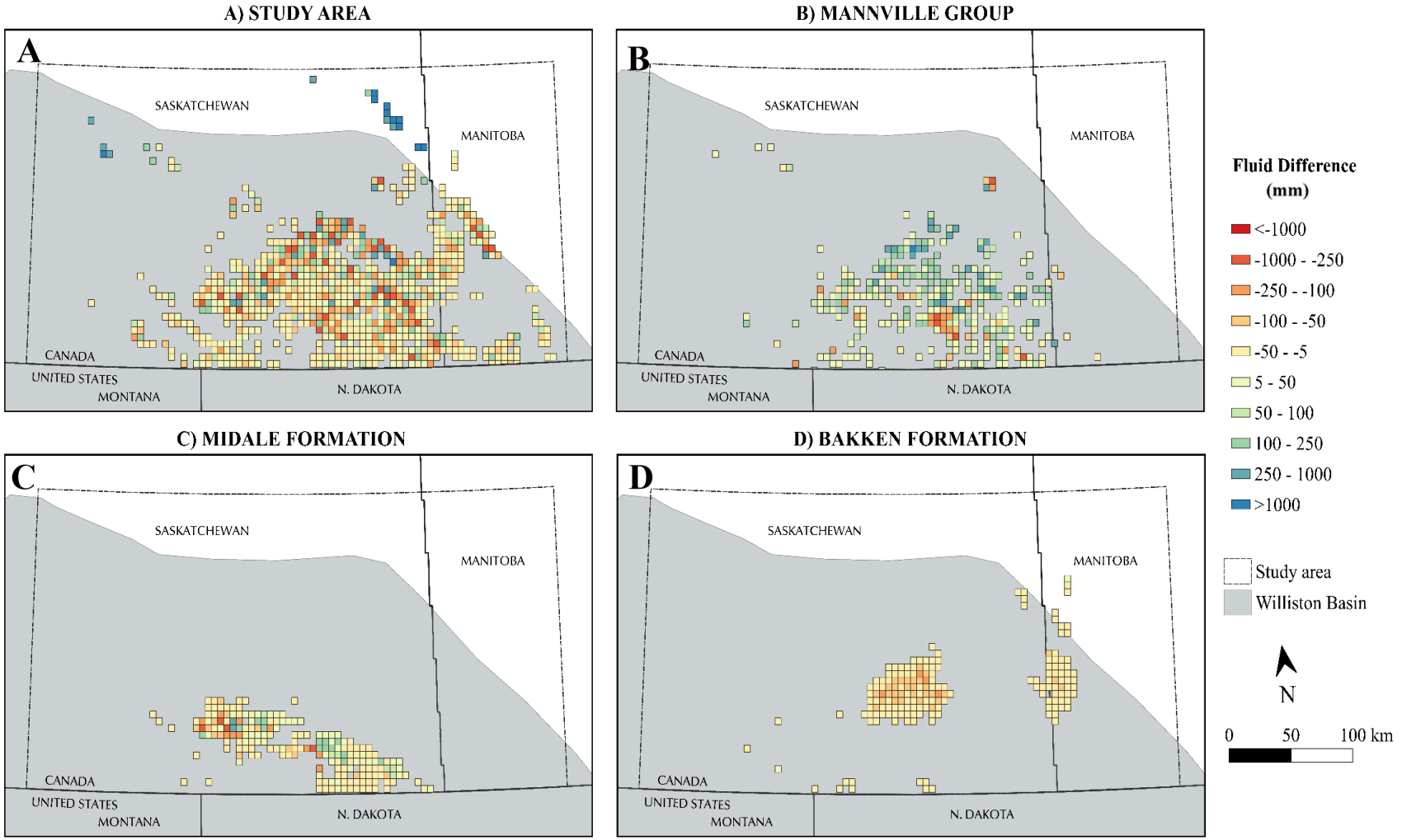

Figure 5-5: Difference in produced and injected volumes. A) By examining the cumulative production and injected volumes for every well in the study area is easy to see the complexity of the system. B) While wells in the Mannville Group are primarily used for injection, there is still many areas that have produced significantly more water. C) produced and injected volumes within the Midale are almost identical, however there are still regions where the difference in these volumes is quite large. D) Since most Bakken wells are hydraulically fractured there is little injected water resulting in every cell having a negative fluid volume change.

5.4 Injection compared to regional flow rates

To quantify the volume of fluid being injected into reservoirs, the annual net fluid budget increase for individual cells was compared to the estimated natural flow rates for each formation. The flow rates occurring in each formation were estimated using Darcy's Law as discussed in Section 4.3. Hydraulic gradients were calculated from hydraulic head maps published by Palombi in 2008, and are based on earlier, pre-development data. The hydraulic gradient in the Midale Member was 0.08 m/km, and the 0.2 m/km in the Midale Group. IRIS (www.saskatchewan.ca/iris) was used to provide thicknesses for each formation. The Midale had a thickness of 18 m, and the Mannville had a thickness of 140 m. A hydraulic conductivity of 1.4×10^{-7} m/s was assumed for the Midale, and an average of 8×10^{-6} m/s was used for the Mannville (MDH Engineered Solutions 2011).

The estimated natural flow rates for each cell in the Midale Member was ~30 m^3/yr, while the Mannville Group was estimated at ~ 35,000 m^3/yr. The significantly larger value for the Mannville compared to the Midale is due to it having a higher permeability and being ten times thicker. The five cells with the injected rates were calculated for both units. Injection volumes ranged from 80,000 to 195,000 m^3/yr in the Midale, and between 240,000 to 1,050,000 m^3/yr in the Mannville. These equate to 2,500 to 6,000 times the background natural flow rates in the Midale, and 7 to 30 times in the Mannville.

6. Modelling Reservoir Pressure

Reservoir pressure models were created for both the Mannville Group and the Midale Member. A model of the Bakken Formation was not created due to its primary method of production being HVHF and its lack of wells with long-term sustained injection rates. Modelling low permeability hydraulically fractured reservoirs and the fluid flow in such environments is too complex for Aqtesolv.

Midale Member

The model for the Midale Member was centered on the injection well with the largest injection volume within the Midale. The chosen well had injected a total of 6.6 x 10^6 m^3 of water between 1963 and 2019 at an average rate of 320 m^3/day. An area of 5 km by 5 km was chosen to allow for an adequate number of wells to interact with the primary injection well. Within the modelled area, there was a total of 124 wells, 110 are used primarily for production, and 14 are used primarily for injection. Since 1957 a total of 50.2 x 10^6 m^3 of fluid was produced, and 42.4 x 10^6 m^3 of fluid was injected in the modelled area. While the total volume of fluid produced is greater than the volume injected, the daily rates follow similar trends (Figure 6-1).

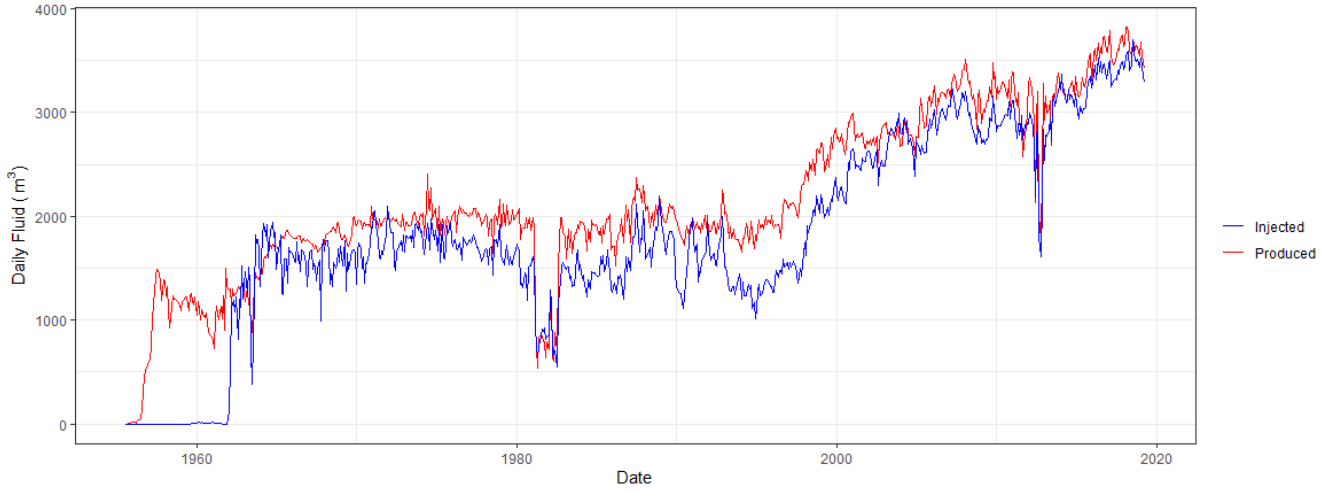

Figure 6-1: Combined daily production (red) and injection (blue) rates (m3) in the Aqtesolv model area for the Midale Member

To accurately model the reservoir response to production and injection, transmissivity and storativity values were calculated from found compressibility, permeability and thickness values (Table 1). The compressibility and permeability of the reservoir came from literature on the

pressure characterizations of the Midale Unit (Beliveau 1989). The thickness was pulled from the drilling records for the primary injection well. From these values, a transmissivity of 2.5 x 10^{-6} m^2/s, and a storativity of 1.6 x 10^{-5} were calculated.

Table 6-1: Model parameters for estimating reservoir pressure changes in the Midale Member

Parameter		Value	Reference
Compressibility	α	1.5 x 10^{-6} kPa^{-1}	Beliveau, 1989
Permeability	k	15 md	Beliveau, 1989
Gross Thickness	b	18 m	IRIS, 2020
Water Density	pw	1076 kg/m^3	IHS Markit, 2020
Dynamic Viscosity	μ	0.001052 Pa·s	Beliveau, 1989
Porosity	n	0.12	IHS Markit, 2020
Hydraulic Conductivity	K	1.4 x 10^{-7} m/s	MDH, 2011
Transmissivity	T	2.5 x 10^{-6} m^2/s	Eq 6
Storativity	S	1.6 x 10^{-5}	Eq 3, 4

Injection wells in the modelled area were arranged in a grid pattern along lines that ran NW-SE and SW-NE (Figure 6-2). Spread amongst these injection wells are production wells that follow no organized pattern. Towards the SW corner of the modelled area is the outer edge of the oil field; due to this, there are no injection wells in this area.

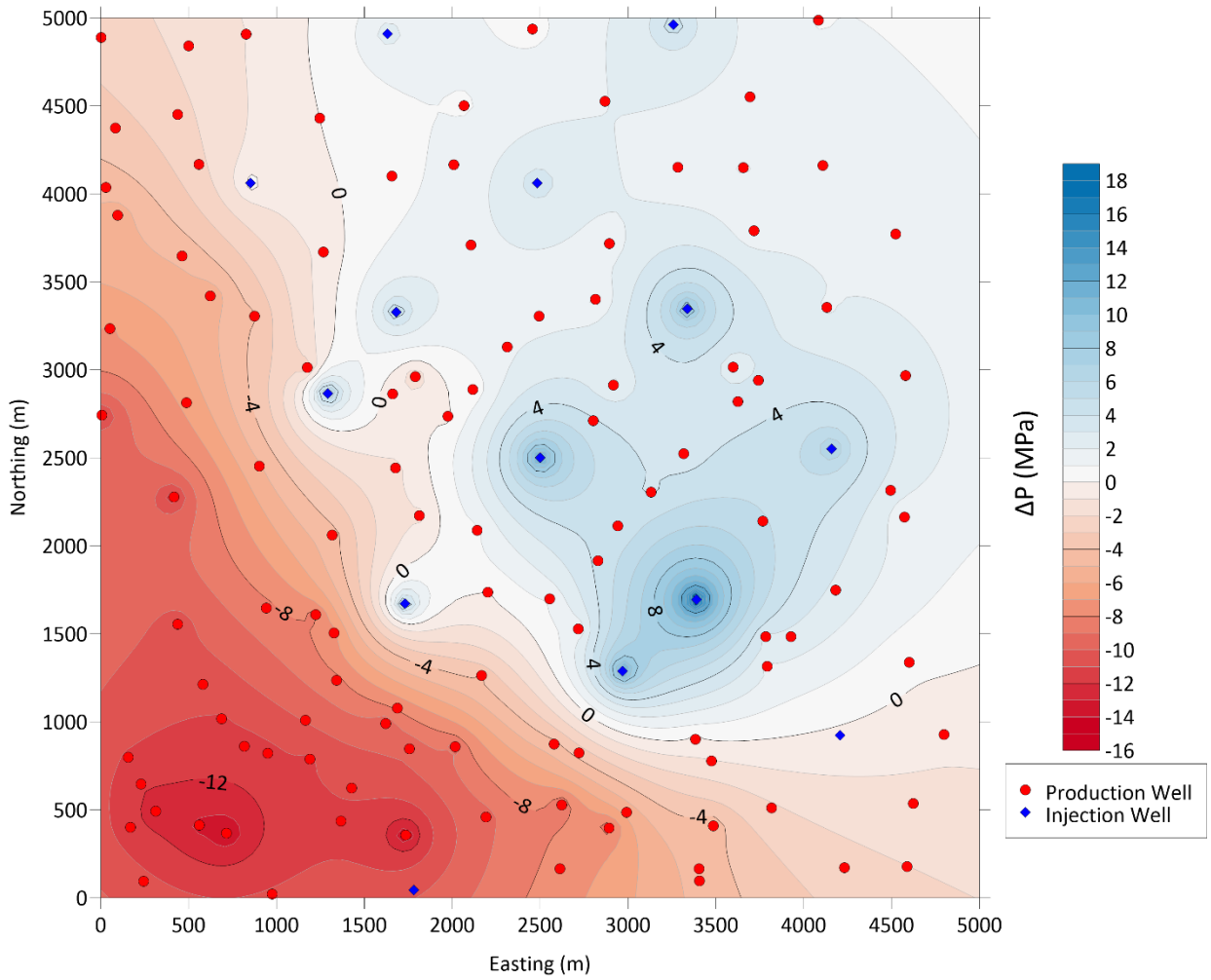

Figure 6-2: Changes in simulated reservoir pressure (ΔP) in the Midale Member. Blue shading represents areas of increased pressure, and red shading represents areas of decreased pressure. T = 2.5 x 10-6 m2/s, S = 1.6 x 10-5, b = 18 m.

Pressure changes are elevated around areas where injection wells are present but decline along the edge of the oil field where only production wells remain. Pressures in the model area maxed at 16.8 MPa at the wellhead and dropped to -14.4 MPa along the outer edge. Pressures greater than 8 MPa extended up to 250 m away from the well, but the pressure is greater than 4 MPa extended up to 700 m away. This increase in pressure can increase the rate of fluid transport raising the risk of contamination.

While the models used reported variables (K, T, S, thickness) to attempt to accurately predict conditions occurring within the formation, such variables can be highly heterogeneous. To assess the impact of changes in these variables a sensitivity analysis was conducted to assess the

performance of the model. Results of the analysis showed that the model was sensitive to changes in S and specifically T. A magnitude change in T resulted in a similar magnitude change in pressures across the formation (Figure A-2).

Mannville Group

The model for the Mannville Group was centered on the injection well with the largest injection volume within the Mannville. The chosen well had injected a total of 9.4 x 10^6 m^3 of water between 1997 and 2019 at an average rate of 1172 m^3/day. An area of 25 km by 25 km was chosen to allow for an adequate number of wells to interact with the primary injection well. Within the modelled area, there was a total of 47 wells, two being used primarily for production, and 45 used primarily for injection. Since 1997 a total of 0.3 x 10^6 m^3 of fluid was produced, and 82.3 x 10^6 m^3 of fluid was injected in the modelled area. There was zero produced fluid in the study area until late 2018 (Figure 6-3).

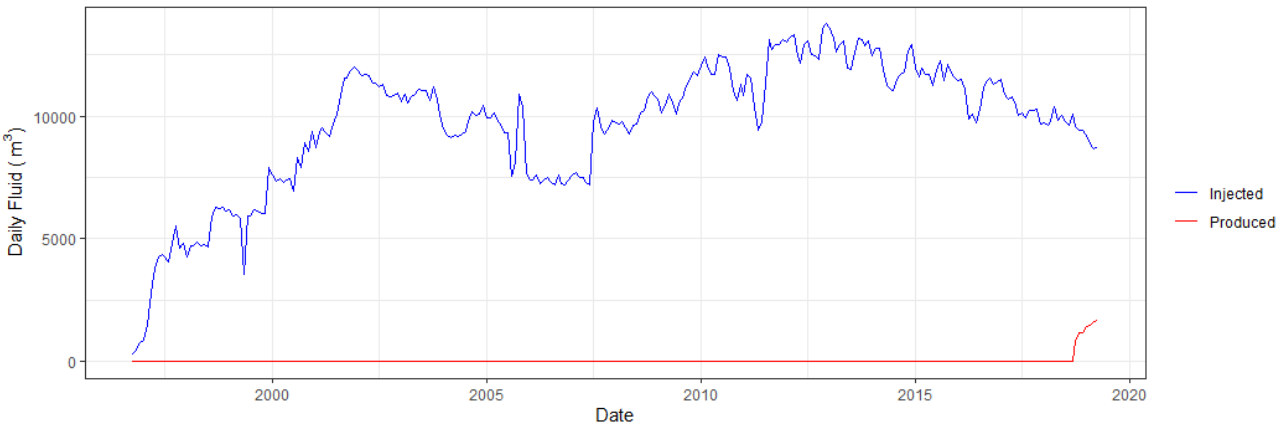

Figure 6-3: Combined daily production (red) and injection (blue) rates (m3) in the Aqtesolv model area for the Mannville Group

Transmissivity and storativity values were calculated from existing hydraulic conductivity, compressibility, permeability and thickness values (Table 2). The reservoir parameters came from a report on a proposed injection well pattern into the Mannville Group (MDH Engineered Solutions 2011); the thickness was pulled from the drilling records for the primary injection well. From these values, a transmissivity of between 1 x 10^{-3} and 1 x 10^{-4} m^2/s, and a storativity of between 1 x 10^{-3} and 1 x 10^{-4} were used.

Table 6-2: Model parameters for estimating reservoir pressure changes in the Mannville Group

Parameter		Value	Reference
Compressibility	α		
Permeability	k	45 md	IHS Energy, 2020
Gross Thickness	b	140 m	IRIS, 2020
Water Density	pw	1022 kg/m^3	IHS Markit, 2020
Dynamic Viscosity	μ	0.001052 Pa·s	Beliveau, 1989
Porosity	n	0.23	IHS Markit, 2020
Hydraulic Conductivity	K	7 x 10^{-6} to 7 x 10^{-7} m/s	MDH, 2011
Transmissivity	T	1 x 10^{-3} to 1 x 10^{-4} m^2/s	MDH, 2011
Storativity	S	1 x 10^{-3} to 1 x 10^{-4}	MDH, 2011

Wells in the Mannville Group are much more spread out in the Midale, and wells are commonly spread up to 5 km apart compared to just a few hundred meters. While wells in the Mannville injected fluid at a much higher rate than those in the Midale, the transmissivity and storativity are much higher, leading to a lower change in pressure across the formation. By using a transmissivity of 1 x 10^{-4} m^2/s, and a storativity of 1 x 10^{-4}, we find a max pressure change of 4.4 MPa. At the wellhead with the minimum increase of 1.25 MPa. Using a transmissivity of 1 x 10^{-3} m^2/s, and a storativity of 1 x 10^{-3}, we find a max pressure change of 0.44 MPa. At the wellhead with the minimum increase of 0.13 MPa (Figure 6-4). The injection wells in the Manville have a much larger area of influence compared to that of the Midale. Significant pressure changes of up to two MPa can be found at up to 15 km away from the centre cluster wells. Modelled sensitivities to changes in S and T can be found in the appendix (Figure A-3).

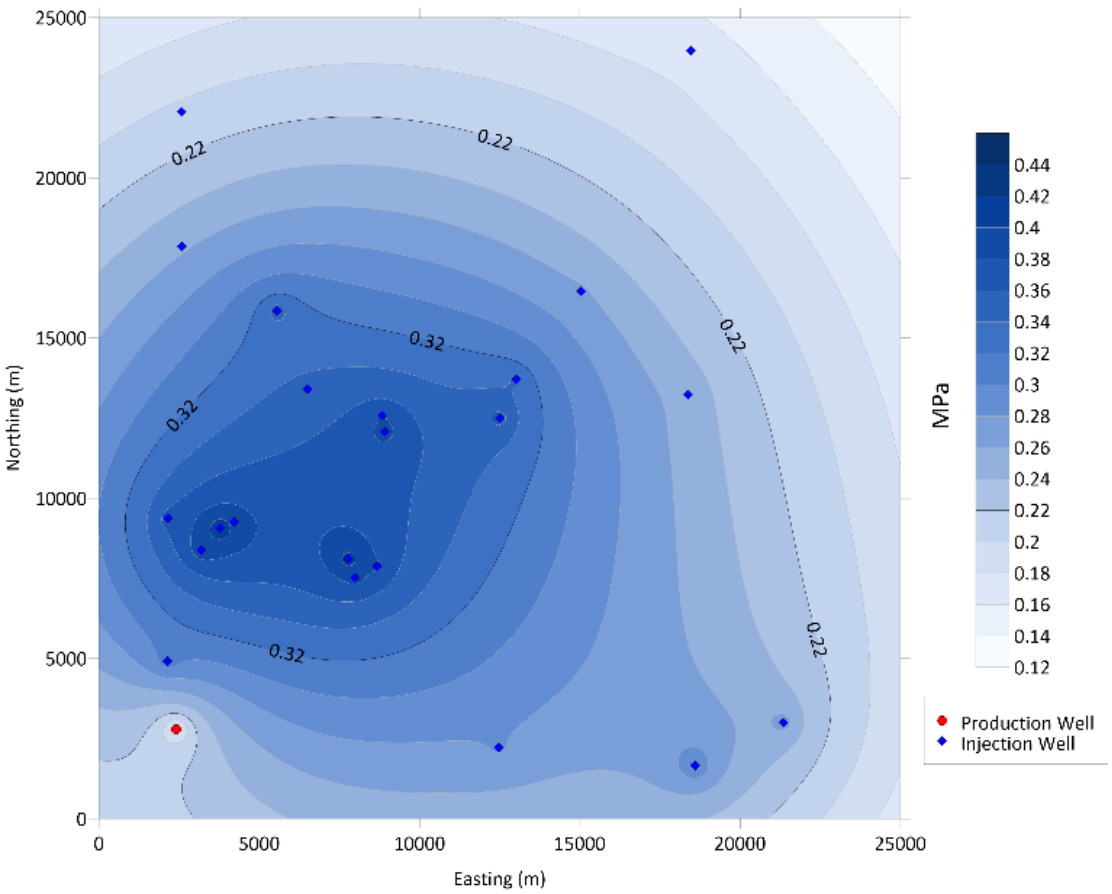

Figure 6-4: Changes in simulated reservoir pressure (ΔP) in the Mannville Group. Blue shading represents areas of increased pressure. T = 1 x 10-3 m2/s, S = 1 x 10-3, b = 120 m.

7. Discussion

7.1 Formational Fluid Volume Change

It is difficult to determine any pattern in fluid volume changes when considering all formations, due to the seemingly random nature of fluid volume distributions (Figure 5-5). Cells with substantial increases in fluid volume can exist directly next to cells with large decreases in fluid volume. To fully understand the effects that oil and gas activities are having on deep groundwater, it is necessary to examine these volumes for individual stratigraphic units.

Since the Mannville Group is used primarily for saltwater disposal, the map in Figure 5-5 mainly shows substantial increases in fluid volumes for most of the cells. Areas where the Mannville Group is used as source water for water flooding, can be seen on the map as a sizeable orange-red area towards the bottom of the Mannville wells. This area of decreased fluid coincides with an area of the Midale Member that has increased in fluid volume, suggesting that within this area, water from the Mannville Group is extensively used for water flooding in the Midale. This provides an example of the formational movement of water that is likely occurring in many other regions across the study area.

Although the difference in the Midale Member between produced and injected fluids is insignificant, (<0.05% of injected volume) it is still possible to see regions of increased fluid volumes as well as decreased fluid volumes. This is due to water flooding, as some cells see more water injected into them to drive oil into the neighbouring cell, as well as cases where water from the Mannville Group is injected into the Midale Member increasing fluid volumes. The majority of cells have a minor amount of fluid volume change, suggesting that in most cases the amount of water injected for water flooding is similar to the amount of water produced, effectively cancelling out the net effect of either.

Oil and gas production in the Bakken Formation is primarily conducted using HVHF which uses substantially less water for production compared to more conventional methods such as water flooding occurring in the Midale Member. This is created a decrease in fluid volume for every cell within the Bakken Formation. Fluid decreases are lower and more consistent than those found in the Mannville Group and the Midale Member.

7.2 The Effect of Oil and Gas on Reservoir Pressures

While assessing produced and injected water volumes on a formational basis is important, it is also imperative to understand how the spatial distribution of production and injection wells affects the subsurface flow and formation pressures. Formations that have total neutral fluid budgets (volumes of produced water equal injected water) can still have regions where there is a significant difference in produced and injected volumes. These differences can be caused by areas where only conventional production is occurring, and no water is being injected, areas where there is no oil present and saltwater disposal is being utilized, and during waterflooding where patterns of injection wells are used to push water and oil towards a series of producing wells. These localized differences in fluid budgets can be seen in the Midale. It is a reservoir with a negligible difference in produced and injected water, yet it has a grid cell with a water surplus of 416 mm/m^2 directly next to a grid cell with a deficit of -255 mm/m^2 (Figure 5-5).

With changes in fluid volume comes changes in formation pressure. Areas with extensive injection will see increases in formation pressures, while areas with more production will see a decrease in pressure. The pressure will fluctuate with the distribution of production and injection wells, sometimes over as little as 100 m. These pressure changes can potentially act as drivers of fluid flow and could lead to contamination of overlying freshwater resources where high permeability pathways are present (McIntosh and Ferguson 2019). Modelled pressures in the Midale showed an increase of >8 MPa up to 250 m away from the injection well, and 2 MPa increases at up to 1.5 km away (Figure 6-2). Due to the variability in hydrogeologic properties, these actual pressure increases may vary within approximately an order of magnitude, although larger pressure increases are unlikely because they would result in hydraulic fracturing. Simulated pressure increases are enough to drive the hydraulic head in the Midale far above the ground surface, causing a risk of near-surface groundwater contamination (Figure 7-1). Unlike hydraulic fracturing, which only increases formation pressures for a few days, pressures due to injection and saltwater disposal can persist for >10 years even after considerable reductions in injection rates (Pollyea et al. 2019).

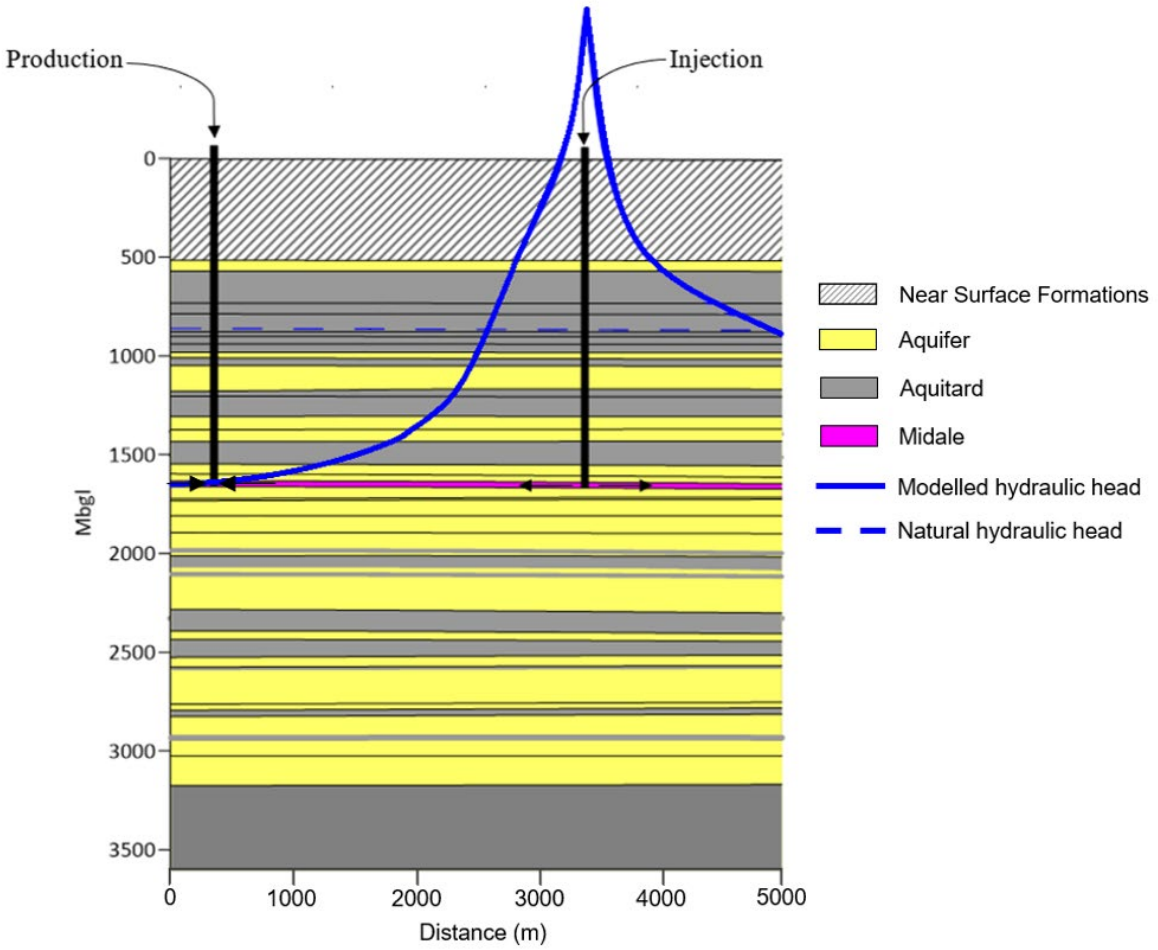

Figure 7-1: Cross-section of hydraulic heads in the Midale. The solid blue line is the modelled hydraulic head due to injection and production, and the dashed blue line is an estimated natural hydraulic head.

The variation in production and injection locations and associated changes in pressure influence the hydraulic gradient of the reservoir, making it difficult to predict groundwater flow direction and velocity. Increased hydraulic gradients will also increase contaminant transport distances where high permeability pathways are present. In areas where natural fractures or faults are absent, leaking abandoned oil and gas wells may act as conduits for contaminant transport. Contamination from leaking wells is not a new phenomenon (Lavasani et al. 2015; Boothroyd et al. 2016), and potential increases in contaminant transport distances will only exacerbate the problems.

7.3 The Role of Pressure in Induced Seismicity

Over the last decade, discussions about induced seismicity have primarily focused on hydraulic fracturing. While induced seismicity can be directly tied to several hydraulic fracturing operations, most induced seismicity in the United States is due to saltwater disposal into deep reservoirs (Rubinstein and Mahani 2015). Several studies have shown that it is possible to induce seismicity via saltwater disposal, and a substantial change in the net fluid budget is the largest influence of seismicity (National Research Council 2013). It is estimated that an increase of as little as 0.01 to 0.2 MPa along faults or tectonically stressed features can induce seismicity (Keranen and Weingarten 2018; Hornbach et al. 2016).

Induced seismicity as a result of large-scale saltwater disposal has been extensively studied in Kansas and Oklahoma. In this region, high volumes are injected into the Arbuckle Group, a thick sedimentary reservoir overlying the crystalline basement. An annual total of 16 million m^3 of wastewater was injected into the Arbuckle in 2015, leading to recorded reservoir pressure increases of up to 0.4 MPa by 2016 (Peterie et al. 2018). This pressure led to a record number of Magnitude 3 earthquakes recorded by the US Geological Survey (USGS) in 2014. Similarities can be found in the Mannville group reservoir, which is primarily used for saltwater disposal. In the Mannville in 2015, there were more than 43 million m^3 of wastewater injected, nearly three times more than in the Arbuckle. This led to modelled increases in the pressure of up to 0.4 MPa around injection wells in the Mannville. Despite these similarities, there are no recorded events of induced seismicity associated with injection into the Mannville.

Reservoirs like the Mannville Group are unlikely to exhibit induced seismicity due to several factors. (1) aquifers properties allow for large influxes of wastewater without a significant increase in reservoir pressure, (2) lack of faults and low shear stress, and (3) distance from the crystalline basement rocks.

The reservoir's response to saltwater disposal depends on several geological constraints, such as thickness, permeability and porosity. Thick, high permeability formations, such as the Manville group, will have high storativity and transmissivity values allowing for a large change in the volume of water storage per unit change in hydraulic head in the aquifer. A smaller change in the hydraulic head will reduce the associated changes in reservoir pressure limiting the chance of induced seismicity.

As wastewater is injected into the reservoir it can propagate down networks of pre-existing fractures and faults. This can modify the state of the stress by increasing the porewater pressure in the fault (Hsieh 1996; National Research Council and Geophysics Study Committee 1990). This reduces the effective stress present on the fault bringing it closer to the conditions required for initiating a slip. This method of induced seismicity can create earthquakes up to magnitude M3.4 (National Research Council 2013).

Wastewater injection into formations that are closer to the crystalline basement of the basin is more likely to induce earthquakes than injection in shallower reservoirs for enhanced oil recovery or hydraulic fracturing (Zhang et al. 2013; Shirzaei et al. 2016). This is caused by the propagation of increased reservoir pressures into the crystalline basement through faults and fracture networks that act as permeable pathways. The increased stresses and frictions found in faults in the crystalline basement will increase the energy released during induced seismicity, resulting in larger earthquakes. Due to the lack of saltwater disposal close to the crystalline basement in the Williston basin, there is no significant induced seismicity recorded.

7.4 Anthropogenic Evolution of Flow

Maps of hydraulic heads exist for nearly every formation. However, most maps are based on natural hydraulic heads, and often remove data that is considered influenced by injection and production wells (Tóth and Corbet 1987). As the results of this study show, production and injection wells will have a significant effect on the hydraulic gradients of reservoirs and will affect groundwater flow estimates and calculations. In addition to changing hydraulic gradients, a surplus produced water is being reinjected into reservoirs at rates significantly higher than natural flow rates, with rates as high as 6,000 times natural flow rates present in the Midale, and up to 30 times in the Mannville. It can no longer be assumed that the subsurface remains in a natural state.

The shift in fluid pressures will make it difficult for projects, such as carbon sequestration, that rely on hydraulic head maps to estimate flow volumes and velocities. To accurately predict reservoir conditions modelling will need to be conducted at each project site, or new basin-wide hydraulic head maps will need to be created with the effect of oil production included. To create basin-wide models of potentiometric surfaces, it will be necessary to model every oil and gas well in the basin. To accurately predict and model long-term forecasting of these potentiometric

surfaces, increases in the reporting of well pressures and volumes must occur. Currently, reservoir pressure measurements only occur before production starts creating a sparse dataset.

8. Conclusion & Recommendations

The continuing rise of oil and gas production has increased the volumes of produced and injected water associated with the oil and gas industry. While it is assumed that most produced water is reinjected into its original source formations, water can often be produced from one formation as source water for injection into a different reservoir to maintain reservoir pressure. It can also be produced as a by-product of production and injected via saltwater disposal into another formation, rather than be injected back into the same formation. This can cause surpluses or deficits in the formation's fluid budget leading to changes in reservoir pressure, increased solute transport and, in some cases, induced seismicity. This study has shown that despite there being negligible differences in produced and injected water volumes in the Williston Basin, there are several formations with large differences in water volumes. In addition to individual formations, the distribution of production and injection wells can lead to local changes in the hydraulic head. Changes in the hydraulic head can act as important drivers of fluid flow, leading to contamination of overlying freshwater resources where high permeability pathways are present.

Several studies have shown that it is possible to induce seismicity due to increases in the hydraulic head via saltwater disposal and that a substantial change in the net fluid budget is the largest influence of seismicity. By modelling pressure changes in the Midale and Mannville, changes in the local hydraulic head were quantified. In the Midale pressure changes were found to exceed >8 MPa at up to 250 m away from the injection well, and 2 MPa at up to 1.5 km away. Increased formation pressures of a similar magnitude have been recorded in other oil and gas producing regions, including Oklahoma, Texas, and Kansas, in some cases leading to induced seismicity. The lack of induced seismicity in the Midale Member and Mannville Group can likely be attributed to a shallower injection distant from the basement.

To further improve the understanding of the rearrangement of fluid flow systems at the basin scale due to oil and gas production, it is recommended that additional data needs to be collected to supplement currently available data. Increasing the required number of fluid pressure measurements for each well and requiring the reporting of the source of injected waters will improve the ability to predict changes in subsurface pressures. Expanding the number of available hydrogeological measurements (permeability, compressibility, porosity, etc) can increase the accuracy of hydraulic head and associated pressure models. Implementing the

collection of multiple fluid chemistry measurements over a well's lifespan instead of only at the time of completion could be useful in tracking the movement of injected fluids.

References

Ahern, J L, and S R Mrkvicka. 1984. “A Mechanical and Thermal Model for the Evolution of the Williston Basin.” *Tectonics* 3 (1): 79–102. https://doi.org/10.1029/TC003i001p00079.

Alberta Energy. 2015. “Let’s Talk About Saskatchewan.”

Anna, L O, Richard Pollastro, and S B Gaswirth. 2010. “Williston Basin Province—Stratigraphic and Structural Framework to a Geologic Assessment of Undiscovered Oil and Gas Resources.” *Assessment of Undiscovered Oil and Gas Resources of the Williston Basin Province of North Dakota, Montana, and South Dakota*.

Bachu, Stefan, and Brian Hitchon. 1996. “Regional-Scale Flow of Formation Waters in the Williston Basin.” *AAPG Bulletin* 80 (2): 248–64. https://doi.org/10.1306/64ed87a0-1724-11d7-8645000102c1865d.

Beliveau, Dennis. 1989. “Pressure Transients Characterize Fractured Midale Unit.” *Journal of Petroleum Technology* 41 (12): 1354–62. https://doi.org/10.2118/15635-PA.

Betcher, R., Christian Pupp, and Gary Grove. 1995. *Groundwater in Manitoba: Hydrogeology, Quality Concerns, Management*. Environment Canada, National Hydrology Research Institute.

Bezys, R K, and G G Conley. 1998. “Geology of the Silurian Interlake Group in Manitoba.” *Stratigraphic Map Series., SI* 1 (1): 200000.

Birdsell, Daniel T, Harihar Rajaram, David Dempsey, and Hari S Viswanathan. 2015. “Hydraulic Fracturing Fluid Migration in the Subsurface: A Review and Expanded Modeling Results.” *Water Resources Research* 51 (9): 7159–88. https://doi.org/10.1002/2015WR017810.

Boothroyd, I M, S Almond, S M Qassim, F Worrall, and R J Davies. 2016. “Fugitive Emissions of Methane from Abandoned, Decommissioned Oil and Gas Wells.” *Science of the Total Environment* 547: 461–69.

Brantley, Susan L, Dave Yoxtheimer, Sina Arjmand, Paul Grieve, Radisav Vidic, Jon Pollak, Garth T Llewellyn, Jorge Abad, and Cesar Simon. 2014. “Water Resource Impacts during

Unconventional Shale Gas Development: The Pennsylvania Experience." *International Journal of Coal Geology* 126: 140–56. https://doi.org/https://doi.org/10.1016/j.coal.2013.12.017.

Carpenter, Alden B. 1978. "Origin And Chemical Evolution Of Brines In Sedimentary Basins." *SPE Annual Fall Technical Conference and Exhibition*. Houston, Texas: Society of Petroleum Engineers. https://doi.org/10.2118/7504-MS.

Christopher, J E. 2003. "Jura-Cretaceous Success Formation and Lower Cretaceous Mannville Group of Saskatchewan." *Report* 223.

Christopher, J E, and M Yurkowski. 2004. "Geological Mapping of Mesozoic Strata in Southeastern Saskatchewan , Northwestern North Dakota , and Northeastern Montana , and Regional Effects of Deformation by Glacial-Ice Loading (IEA Weyburn CO 2 Monitoring and Storage Project)" 1: 1–20.

Clark, C E, and J A [Environmental Science Division] Veil. 2009. "Produced Water Volumes and Management Practices in the United States." United States. https://doi.org/10.2172/1007397.

Connolly, Cathy A, Lynn M Walter, H Baadsgaard, and Fred J Longstaffe. 1990. "Origin and Evolution of Formation Waters, Alberta Basin, Western Canada Sedimentary Basin. I. Chemistry." *Applied Geochemistry* 5 (4): 375–95. https://doi.org/https://doi.org/10.1016/0883-2927(90)90016-X.

Darrah, Thomas H., Robert B Jackson, Avner Vengosh, Nathaniel R Warner, Colin J Whyte, Talor B Walsh, Andrew J Kondash, and Robert J Poreda. 2015. "The Evolution of Devonian Hydrocarbon Gases in Shallow Aquifers of the Northern Appalachian Basin: Insights from Integrating Noble Gas and Hydrocarbon Geochemistry." *Geochimica et Cosmochimica Acta* 170: 321–55. https://doi.org/https://doi.org/10.1016/j.gca.2015.09.006.

DMR (North Dakota Mineral Resources). 2019. "Oil and Gas in North Dakota - Fact Sheet."

Downey, Joe S, John F Busby, and George A Dinwiddie. 1987. "Regional Aquifers and Petroleum in the Williston Basin Region of the United States." *AAPG Bulletin*, 299–312.

Ferguson, Grant. 2015. "Deep Injection of Waste Water in the Western Canada Sedimentary

Basin." *Groundwater* 53 (2): 187–94. https://doi.org/10.1111/gwat.12198.

Ferguson, Grant, R. Betcher, and Stephen E Grasby. 2006. "Hydrogeology of the Winnipeg Formation in Manitoba, Canada." *Hydrogeology Journal* 15 (3): 573. https://doi.org/10.1007/s10040-006-0130-4.

Ferguson, Grant, and Stephen E Grasby. 2014. "The Geothermal Potential of the Basal Clastics of Saskatchewan, Canada." *Hydrogeology Journal* 22 (1): 143–50. https://doi.org/10.1007/s10040-013-1061-5.

Ferguson, Grant, Jennifer C McIntosh, Stephen E Grasby, M Jim Hendry, Scott Jasechko, Matthew B J Lindsay, and Elco Luijendijk. 2018. "The Persistence of Brines in Sedimentary Basins." *Geophysical Research Letters* 45 (10): 4851–58. https://doi.org/10.1029/2018GL078409.

Gallegos, Tanya J, Brian A Varela, Seth S Haines, and Mark A Engle. 2016. "Assessment of a Numerical Model to Reproduce Event-Scale Erosion and Deposition Distributions in a Braided River." *Water Resources Research*, no. 52: 6621–42. https://doi.org/10.1002/2015WR017278.Received.

Gerhard, Lee C, Sidney B Anderson, Julie A Lefever, and Clarence G Carlson. 1982. "Geological Development, Origin, and Energy Mineral Resources of Williston Basin, North Dakota1." *AAPG Bulletin* 66 (8): 989–1020. https://doi.org/10.1306/03B5A62E-16D1-11D7-8645000102C1865D.

Golden Software LLC. 2020. "Surfer."

Grasby, Stephen E, Kirk Osadetz, R. Betcher, and Frank Render. 2000. "Reversal of the Regional-Scale Flow System of the Williston Basin in Response to Pleistocene Glaciation." *Geology* 28 (7): 635–38. https://doi.org/10.1130/0091-7613(2000)28<635:ROTRFS>2.0.CO;2.

Hannon, Norbert. 1987. "Subsurface Water Flow Patterns in the Canadian Sector of the Williston Basin." *AAPG Bulletin*, 313–22.

Hanor, Jeffrey S. 1994. "Origin of Saline Fluids in Sedimentary Basins." *Geological Society, London, Special Publications* 78 (1): 151 LP – 174.

https://doi.org/10.1144/GSL.SP.1994.078.01.13.

Hendry, M Jim, S L Barbour, K Novakowski, and L I Wassenaar. 2013. “Paleohydrogeology of the Cretaceous Sediments of the Williston Basin Using Stable Isotopes of Water.” *Water Resources Research* 49 (8): 4580–92. https://doi.org/10.1002/wrcr.20321.

Hitchon, Brian, Gale K Billings, and J E Klovan. 1971. “Geochemistry and Origin of Formation Waters in the Western Canada Sedimentary Basin—III. Factors Controlling Chemical Composition.” *Geochimica et Cosmochimica Acta* 35 (6): 567–98. https://doi.org/https://doi.org/10.1016/0016-7037(71)90088-3.

Hoganson, John W. 1978. “Microfacies Analysis and Depositional Environments of the Duperow Formation (Fransnian) in the North Dakota Part of the Williston Basin.” In *Montana Geological Society 24th Annual Conference*, 134–44. Montana Geological Society.

Hornbach, Matthew J, Madeline Jones, Monique Scales, Heather R DeShon, M Beatrice Magnani, Cliff Frohlich, Brian Stump, Chris Hayward, and Mary Layton. 2016. “Ellenburger Wastewater Injection and Seismicity in North Texas.” *Physics of the Earth and Planetary Interiors* 261: 54–68. https://doi.org/https://doi.org/10.1016/j.pepi.2016.06.012.

Horner, R M, C B Harto, R B Jackson, E R Lowry, A R Brandt, T W Yeskoo, D J Murphy, and C E Clark. 2016. “Water Use and Management in the Bakken Shale Oil Play in North Dakota.” *Environmental Science & Technology* 50 (6): 3275–82. https://doi.org/10.1021/acs.est.5b04079.

Hsieh, Paul A. 1996. “Deformation-Induced Changes in Hydraulic Head During Ground-Water Withdrawal.” *Groundwater* 34 (6): 1082–89. https://doi.org/10.1111/j.1745-6584.1996.tb02174.x.

Hutchence, K, J H Weston, A G Law, L W Vigrass, and F W Jones. 1986. “Modeling of a Liquid Phase Geothermal Doublet System at Regina, Saskatchewan, Canada.” *Water Resources Research* 22 (10): 1469–79. https://doi.org/10.1029/WR022i010p01469.

HydroSOLVE Inc. 2016. “AQTESOLV.” Reston: HydroSOLVE. www.aqtesolv.com.

IHS Markit. 2020. “IHS AccuMap.” Englewood, Colorado: IHS Markit. https://ihsmarkit.com/products/oil-gas-tools-accumap.html.

Kent, D M, and J E Christopher. 1994. “Geological History of the Williston Basin and Sweetgrass Arch.” In *Geological Atlas of the Western Canada Sedimentary Basin*, edited by G.D Mossop and I Shetsen, 421–29. Canadian Society of Petroleum Geologists and Alberta Research Council. https://ags.aer.ca/publications/chapter-27-williston-basin-and-sweetgrass-arch.html.

———. 2008. “Geological History of the Williston Basin and Sweetgrass Arch.” In *Atlas of The Western Canadian Sedimentary Basin*, 421–29. Alberta Energy Regulator. https://doi.org/10.1016/B978-0-12-374194-3.00027-5.

Keranen, Katie M, and Matthew B. Weingarten. 2018. “Induced Seismicity.” *Annual Review of Earth and Planetary Sciences* 46 (1): 149–74. https://doi.org/10.1146/annurev-earth-082517-010054.

Khan, D K, and B J Rostron. 2005. “Regional Hydrogeological Investigation around the IEA Weyburn CO2 Monitoring and Storage Project Site.” In *Greenhouse Gas Control Technologies 7*, 741–50. Elsevier.

Kiran, Raj, Catalin Teodoriu, Younas Dadmohammadi, Runar Nygaard, David Wood, Mehdi Mokhtari, and Saeed Salehi. 2017. “Identification and Evaluation of Well Integrity and Causes of Failure of Well Integrity Barriers (A Review).” *Journal of Natural Gas Science and Engineering* 45: 511–26. https://doi.org/https://doi.org/10.1016/j.jngse.2017.05.009.

Kondash, Andrew J, Nancy E. Lauer, and Avner Vengosh. 2018. “The Intensification of the Water Footprint of Hydraulic Fracturing.” *Science Advances* 4 (8): eaar5982. https://doi.org/10.1126/sciadv.aar5982.

Lavasani, Seyed Miri, Nahid Ramzali, Farinaz Sabzalipour, and Emre Akyuz. 2015. “Utilisation of Fuzzy Fault Tree Analysis (FFTA) for Quantified Risk Analysis of Leakage in Abandoned Oil and Natural-Gas Wells.” *Ocean Engineering* 108: 729–37. https://doi.org/https://doi.org/10.1016/j.oceaneng.2015.09.008.

Llewellyn, Garth T, Frank Dorman, J L Westland, D Yoxtheimer, Paul Grieve, Todd Sowers, E

Humston-Fulmer, and Susan L Brantley. 2015. “Evaluating a Groundwater Supply Contamination Incident Attributed to Marcellus Shale Gas Development.” *Proceedings of the National Academy of Sciences* 112 (20): 6325 LP – 6330. https://doi.org/10.1073/pnas.1420279112.

Lutz, Brian D, Aurana N Lewis, and Martin W Doyle. 2013. “Generation, Transport, and Disposal of Wastewater Associated with Marcellus Shale Gas Development.” *Water Resources Research* 49 (2): 647–56. https://doi.org/10.1002/wrcr.20096.

Maathuis, H. 2008. “The Quality of Natural Groundwaters in Saskatchewan.” Saskatoon.

McIntosh, Jennifer C, and Grant Ferguson. 2019. “Conventional Oil—The Forgotten Part of the Water-Energy Nexus.” *Groundwater* 57 (5): 669–77. https://doi.org/10.1111/gwat.12917.

McIntosh, Jennifer C, M Jim Hendry, Chris J Ballentine, R S Haszeldine, B. Mayer, G Etiope, M Elsner, et al. 2019. “A Critical Review of State-of-the-Art and Emerging Approaches to Identify Fracking-Derived Gases and Associated Contaminants in Aquifers.” *Environmental Science & Technology* 53 (3): 1063–77. https://doi.org/10.1021/acs.est.8b05807.

McMahon, P B, L N Plummer, J K Böhlke, S D Shapiro, and S R Hinkle. 2011. “A Comparison of Recharge Rates in Aquifers of the United States Based on Groundwater-Age Data.” *Hydrogeology Journal* 19 (4): 779. https://doi.org/10.1007/s10040-011-0722-5.

MDH Engineered Solutions. 2011. “Hydrogeology Mapping of NTS Mapsheet Saskatoon 73B.”

Murray, Kyle E. 2013. “State-Scale Perspective on Water Use and Production Associated with Oil and Gas Operations, Oklahoma, U.S.” *Environmental Science & Technology* 47 (9): 4918–25. https://doi.org/10.1021/es4000593.

Muskat, Morris. 1937. “The Flow of Fluids Through Porous Media.” *Journal of Applied Physics* 8 (4): 274–82. https://doi.org/10.1063/1.1710292.

National Research Council. 2013. *Induced Seismicity Potential in Energy Technologies*. National Academies Press.

National Research Council, and Geophysics Study Committee. 1990. *The Role of Fluids in Crustal Processes*. National Academies Press.

Nicolas, M P B. 2015. “Potash Deposits in the Devonian Prairie Evaporite, Southwestern Manitoba (Parts of NTS 62F, K).” *Report of Activities 2015*.

North Dakota State Industrial Commission. 2020. “Monthly Production Report Index.” Bismarck.

Palombi, Daniele Davide. 2008. “Regional Hydrogeological Characterization of the Northern Margin in the Williston Basin.” University of Alberta. https://doi.org/10.1111/an.1968.9.8.11.3.

Palombi, Daniele Davide, and Ben Rostron. 2006. “Regional Hydrochemistry of Lower Paleozoic Aquifers in the Northern Portion of the Williston Basin, Saskatchewan-Manitoba.”

Pendrigh, Nicole M. 2005. “Geological and Geophysical Characterization of the Mississippian Midale Reservoir, Weyburn Field, Saskatchewan.” *Saskatchewan Geological Survey, Summary of Investigations 2005* 1: 1–16.

Peterie, Shelby L, Richard D Miller, John W Intfen, and Julio B Gonzales. 2018. “Earthquakes in Kansas Induced by Extremely Far-Field Pressure Diffusion.” *Geophysical Research Letters* 45 (3): 1395–1401. https://doi.org/10.1002/2017GL076334.

Peterson, James A, and Lawrence M MacCary. 1987. “Regional Stratigraphy and General Petroleum Geology of the US Portion of the Williston Basin and Adjacent Areas.” *AAPG Bulletin*, 9–44.

Pollyea, Ryan M, Martin C Chapman, Richard S Jayne, and Hao Wu. 2019. “High Density Oilfield Wastewater Disposal Causes Deeper, Stronger, and More Persistent Earthquakes.” *Nature Communications* 10 (1): 3077. https://doi.org/10.1038/s41467-019-11029-8.

Rubinstein, Justin L, and Alireza Babaie Mahani. 2015. “Myths and Facts on Wastewater Injection , Hydraulic Fracturing , Enhanced Oil Recovery , and Induced Seismicity.” *Seismological Research Letters* 86 (4): 1060–1067. https://doi.org/10.1785/0220150067.

Scanlon, Bridget R., R C Reedy, and J.P. Nicot. 2014. “Comparison of Water Use for Hydraulic Fracturing for Unconventional Oil and Gas versus Conventional Oil.” *Environmental Science & Technology* 48 (20): 12386–93. https://doi.org/10.1021/es502506v.

Scanlon, Bridget R., Robert C. Reedy, Matthew B. Weingarten, and Kyle E Murray. 2019. "Managing Basin-Scale Fluid Budgets to Reduce Injection-Induced Seismicity from the Recent U.S. Shale Oil Revolution." *Seismological Research Letters* 90 (1): 171–82. https://doi.org/10.1785/0220180223.

Scanlon, Bridget R., Robert C Reedy, Frank Male, and Mark Walsh. 2017. "Water Issues Related to Transitioning from Conventional to Unconventional Oil Production in the Permian Basin." *Environmental Science & Technology* 51 (18): 10903–12. https://doi.org/10.1021/acs.est.7b02185.

Schlegel, Melissa E, Zheng Zhou, Jennifer C McIntosh, Chris J Ballentine, and Mark A Person. 2011. "Constraining the Timing of Microbial Methane Generation in an Organic-Rich Shale Using Noble Gases, Illinois Basin, USA." *Chemical Geology* 287 (1): 27–40. https://doi.org/https://doi.org/10.1016/j.chemgeo.2011.04.019.

Sherwood, Owen A, Jessica D Rogers, Greg Lackey, Troy L Burke, Stephen G Osborn, and Joseph N Ryan. 2016. "Groundwater Methane in Relation to Oil and Gas Development and Shallow Coal Seams in the Denver-Julesburg Basin of Colorado." *Proceedings of the National Academy of Sciences* 113 (30): 8391–96. https://doi.org/10.1073/pnas.1523267113.

Shirzaei, Manoochehr, William L Ellsworth, Kristy F Tiampo, Pablo J González, and Michael Manga. 2016. "Surface Uplift and Time-Dependent Seismic Hazard Due to Fluid Injection in Eastern Texas." *Science* 353 (6306): 1416 LP – 1419. https://doi.org/10.1126/science.aag0262.

Simpson, Frank, H R McCabe, and D Barchyn. 1987. "Subsurface Disposal of Wastes in Manitoba, Part 1: Current Status and Potential of Subsurface Disposal of Fluid Industrial Wastes in Manitoba." Manitoba Energy and Mines, Geological Services.

Soeder, Daniel J. 2018. "The Successful Development of Gas and Oil Resources from Shales in North America." *Journal of Petroleum Science and Engineering* 163 (August 2017): 399–420. https://doi.org/10.1016/j.petrol.2017.12.084.

Spencer, Ronald J. 1987. "Origin of CaCl Brines in Devonian Formations, Western Canada

Sedimentary Basin." *Applied Geochemistry* 2 (4): 373–84. https://doi.org/https://doi.org/10.1016/0883-2927(87)90022-9.

Tiedeman, Kate, Sonia Yeh, Bridget R. Scanlon, Jacob Teter, and Gouri Shankar Mishra. 2016. "Recent Trends in Water Use and Production for California Oil Production." *Environmental Science & Technology* 50 (14): 7904–12. https://doi.org/10.1021/acs.est.6b01240.

Tóth, J, and T Corbet. 1987. "Post-Palaeocene Evolution of Regional Groundwater Flow Systems and Their Relation to Petroleum Accumulations, Taber Area, Southern Alberta, Canada." *Geological Society, London, Special Publications* 34 (1): 45 LP – 77. https://doi.org/10.1144/GSL.SP.1987.034.01.05.

Veil, John. 2020. "US Produced Water Volumes and Management Practices in 2017."

Vengosh, Avner, Robert B Jackson, Nathaniel R Warner, Thomas H. Darrah, and Andrew J Kondash. 2014. "A Critical Review of the Risks to Water Resources from Unconventional Shale Gas Development and Hydraulic Fracturing in the United States." *Environmental Science & Technology* 48 (15): 8334–48. https://doi.org/10.1021/es405118y.

Warner, Nathaniel R, Cidney A Christie, Robert B Jackson, and Avner Vengosh. 2013. "Impacts of Shale Gas Wastewater Disposal on Water Quality in Western Pennsylvania." *Environmental Science & Technology* 47 (20): 11849–57. https://doi.org/10.1021/es402165b.

Weyer, K Udo, and James C Ellis. 2013. "Long Range Regional Groundwater Flow Systems in the Northern Great Plains : (1) Groundwater Flow Directions within the Midale Formation at the Weyburn Carbon Sequestration Site, Saskatchewan, Canada." *Geo Montreal 2013*.

Whittaker, Steve, and Kyle Worth. 2011. "Aquistore: A Fully Integrated Demonstration of the Capture, Transportation and Geologic Storage of CO2." *Energy Procedia* 4: 5607–14. https://doi.org/https://doi.org/10.1016/j.egypro.2011.02.550.

Wilson, James Lee. 1967. "CARBONATE-EVAPORITE CYCLES IN LOWER DUPEROW FORMATION OF WILLISTON BASIN1." *Bulletin of Canadian Petroleum Geology* 15 (3): 230–312. https://doi.org/10.35767/gscpgbull.15.3.230.

Wu, May, Marianne Mintz, Michael Wang, Salil Arora, and Energy Systems Division. 2009.

"Consumptive Water Use in the Production of Bioethanol and Petroleum Gasoline."

Zhang, Yipeng, Mark Person, John Rupp, Kevin Ellett, Michael A Celia, Carl W Gable, Brenda Bowen, et al. 2013. "Hydrogeologic Controls on Induced Seismicity in Crystalline Basement Rocks Due to Fluid Injection into Basal Reservoirs." *Groundwater* 51 (4): 525–38. https://doi.org/10.1111/gwat.12071.

Appendix

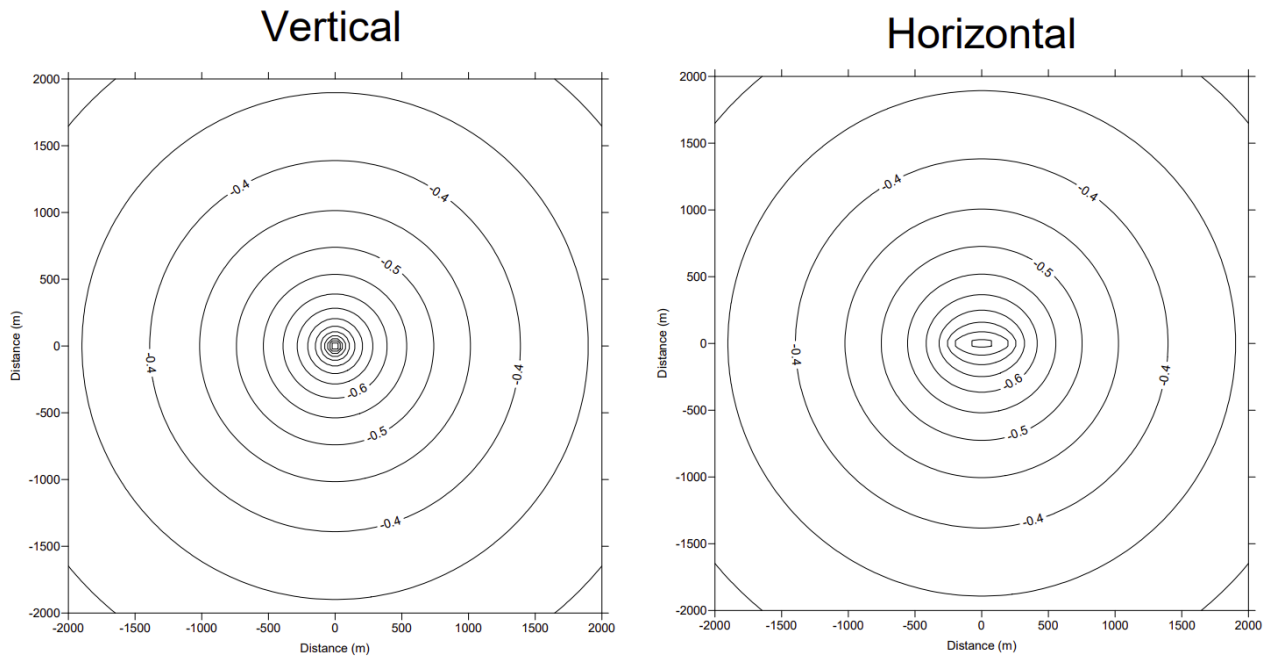

Figure A-1: Variations in modelled pressure due to using vertical wells versus using horizontal wells. Figure uses data from a well present in the Midale study area with a lateral length of 492.1 m. All other variables are consistent with the previous pressure change modelling conducted in the study area. Differences between the two models are primarily focused on 200 meters of the center of the well.

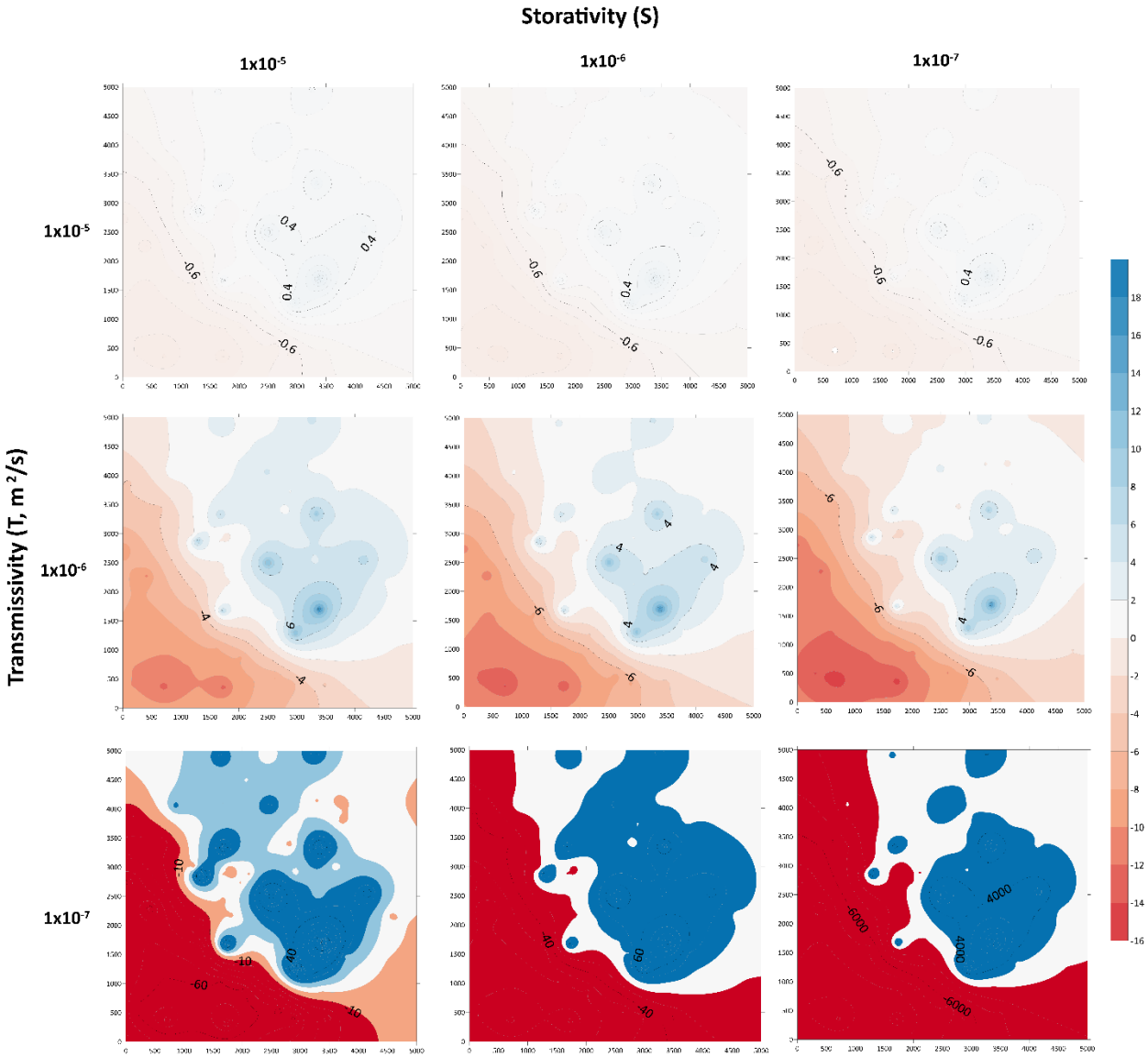

Figure A-2: Sensitivity analysis of variation in Storativity and Transmissivity in the Midale Member

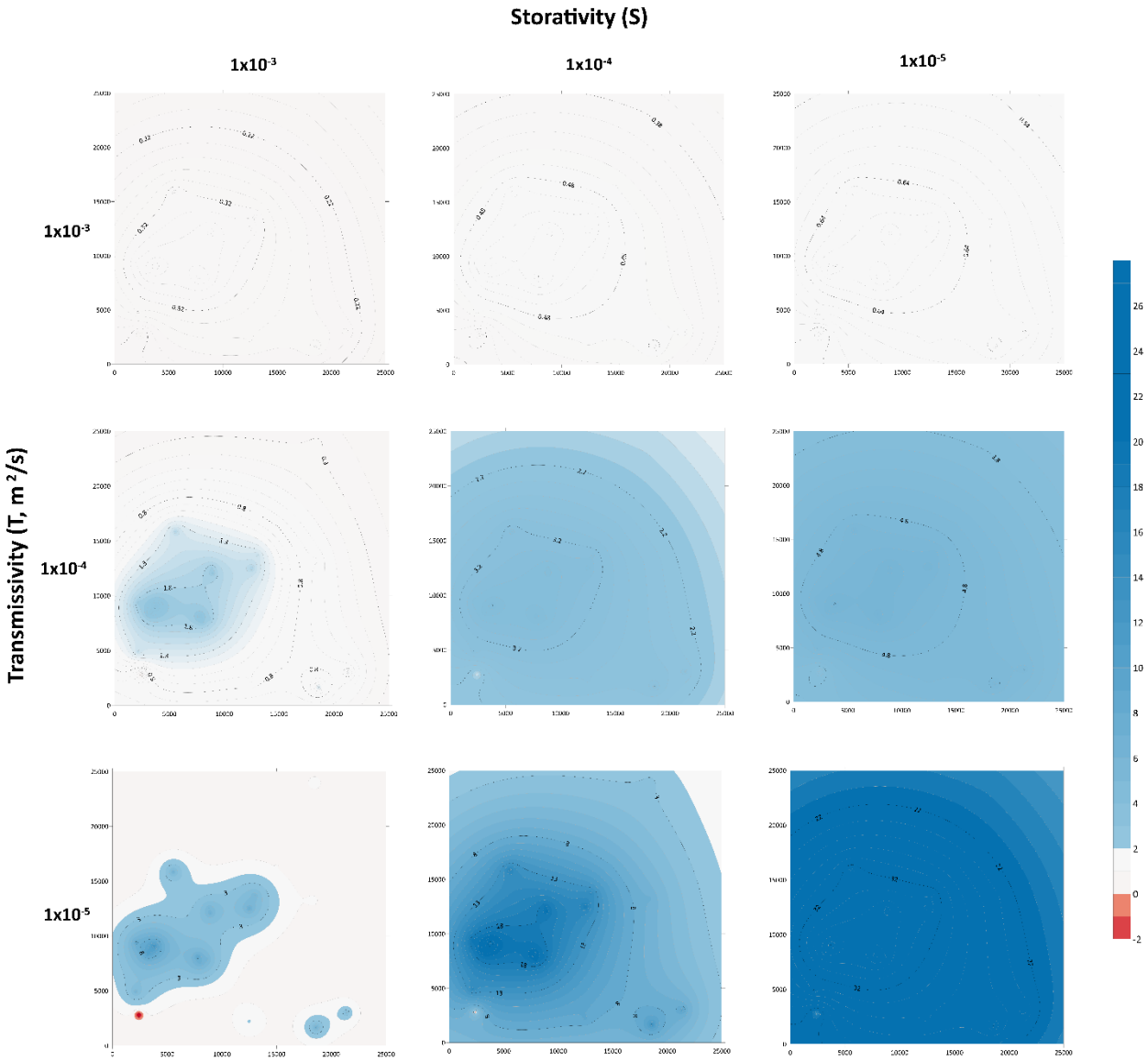

Figure A-3: Sensitivity analysis of variation in Storativity and Transmissivity in the Mannville Group